UNIVERSIDADE D
COIMBRA

Gabriela Correia Barros

Photodynamic therapy as an innovative approach to Endometrial Cancer Stem Cells

Master's thesis in Cellular and Molecular Biology, supervised by Doctor Mafalda Sofia Laranjo Cândido and co-supervised by Doctor Catarina Seabra presented to the Faculty of Science and Technology, University of Coimbra, Coimbra, Portugal

October, 2021

Faculdade de Ciencias e Tecnologia da Universidade de Coimbra

Photodynamic therapy as an innovative approach to Endometrial Cancer Stem Cells

Gabriela Correia Barros

Dissertação no âmbito do Mestrado em Biologia Celular e Molecular orientada pela Investigadora Doutora Mafalda Laranjo e co-orientada pela Investigadora Doutora Catarina Seabra, apresentada à Faculdade de Faculdade de Ciências e Tecnologia da Universidade de Coimbra.

October, 2021

UNIVERSIDADE D
COIMBRA

This work was developed in at:

with the collaboration of:

«"Afinal, a ciência é essencialmente internacional e é somente pela falta de senso histórico que as qualidades da nacionalidade foram atribuídas a ela"»

Marie Curie

Agradecimentos

Mais um fim de um ciclo em minha vida, de mais uma etapa da minha jornada acadêmica e profissional, e gostaria de todo meu coração agradecer a todos que, de alguma forma, foram imprescindíveis não só para esse projeto e para a realização dessa dissertação, mas também por me ajudar com minhas batalhas internas e não me deixar esquecer da minha força, capacidade e motivação.

À Doutora Mafalda Laranjo, investigadora da Faculdade de Medicina da Universidade de Coimbra, orientadora desta tese, agradeço toda a humanidade e ajuda em todos os momentos que precisei. Também agradeço a disponibilidade e atenção de sempre, toda a paciência e didática que fizeram dessa minha jornada mais fácil. Sou muito grata pelo profissionalismo, o rigor e a confiança em mim. De certo, graças a si, posso dizer que desenvolvi um gosto ainda mais especial pela parte de investigação laboratorial dessa área da ciência. Agradeço também todas as correções e sugestões realizadas à esta tese a todo o trabalho de investigação.

À Professora Doutora Maria Filomena Botelho, Professora Catedrática da Faculdade de Medicina da Universidade de Coimbra e diretora do Instituto de Biofísica desta instituição, agradeço a oportunidade de integrar a equipe de investigação por si liderada e à disponibilidade demonstrada.

À Doutora Catarina Seabra, investigadora do Centro de Neurociências e Biologia Celular de Coimbra, orientadora interna deste trabalho, por toda a disponibilidade.

À Doutora Maria João Carvalho, médica especialista em Ginecologia e Obstetrícia no Centro Hospitalar e Universitário de Coimbra (CHUC) e Assistente Convidada da Faculdade de Medicina da Universidade de Coimbra, agradeço todos os ensinamentos e paciência. Agradeço também todas as correções realizadas a este manuscrito.

À Mestre Beatriz Serambeque que também nunca pensou duas vezes antes de me ajudar, explicar e até mesmo acalmar. Obrigada por todos ensinamentos e pela paciência.

Ao Miguel Marto, por me ter acolhido no grupo, ensinado tudo o que sei sobre o laboratório que foi minha casa por mais de um ano, por toda a ajuda indispensável que me foi dada ao longo destes meses.

Aos colegas do laboratório e mestres Catarina Guilherme, Ricardo Teixo e Inês Marques, bem como Ana Dias, Beatriz, Lúcia e Margarida. Obrigada por me acolherem e me fazer sentir que não estive sozinha, que pude tirar as dúvidas que me fizeram ser uma profissional e uma pessoa melhor.

Ao meu porto seguro e mãe, Núbia Correia, à quem agradeço infinitamente por todo apoio e incentivo que tive em toda a minha vida. Quem me espelho e tenho como exemplo de força e sempre ir em busca dos meus sonhos. Obrigada por estar do meu lado em mais uma etapa!

À minha família, que de todas as jornadas do mundo, vocês são quem me motivam, me faz querer ser melhor, acreditar em mim e lembrar que

"eu só quero agradecer
por ter vocês
Pra acompanhar minhas loucuras

Me deixar bem mais segura
Daquilo que eu posso ser se eu somente acreditar
E eu só quero agradecer
mais uma vez
Por me aguentarem insegura,
me tornarem mais madura
E me mostrarem que os sonhos não se devem adiar
Por dar risada de tudo
e sempre colorir meu mundo
Com as cores mais bonitas que eu já vi alguém pintar
Por me amarem com a mesma intensidade
E por serem, de verdade,
a melhor família que eu pudesse ganhar"

Aos meus amigos da UNIRIO, Logosófico e da vida, por estarem sempre comigo independentemente de onde eu estiver. Por me presentear todos os dias com a amizade e carinho, e principalmente com a certeza de que tenho bons comigo.

À minha surpresa e presente dessa minha etapa, Uran. Obrigada por tornar os dias difíceis mais leves, e me fazer lembrar que sempre tenho um bom motivo para sorrir, mesmo quando não está tão claro. Obrigada pela paciência, pelas piadas e por eu não sentir nem um tipo de receio em ser quem exatamente sou.

Ao Horácio, meu querido e amado. Obrigada por estar comigo sempre e não colocar nenhuma condição para me amar!

Outputs

Work presented in the context of this dissertation

Part of the results that make up this dissertation were submitted, accepted and presented as a poster in the

II ASPIC-ASEICA International Meeting – Current Trends in Precision Medicine in Cancer October 2021.

Correia-Barros, G., Serambeque, B., Carvalho, M.J., Pereira, N., Gonçalves, A.C., Pineiro, M., Pinho e Melo, T.M.D.V., Botelho, M.F., Laranjo, M. EVALUATION OF THE EFFECTIVENESS OF PHOTODYNAMIC THERAPY BASED ON NOVEL CHLORINS ON ENDOMETRIAL CANCER

Closely related with this work, the following manuscript is being prepared:

Gabriela Barros*, Beatriz Serambeque*, Maria João Carvalho, Carlos Miguel Marto, Maria Filomena Botelho, Mafalda Laranjo. APPLICATIONS OF PHOTODYNAMIC THERAPY IN ENDOMETRIAL DISEASES. (*Shared first authorship). In preparation to be submitted to Lasers in Surgery and Medicine.

This manuscript reviews the state of the art of the use of PDT in endometrial diseases, from endometrial cancer to benign diseases such as abnormal uterine bleeding or adenomyosis. In this work all studies found using in vitro models, animal studies and clinical trials are reviewed and discussed.

Abstract

Endometrial cancer (EC) represents about 6% of female cancers, being the most frequent gynaecological malignancy in developed countries. Radical surgery is the primary treatment but in young women or patients with higher surgical risk may not be an option. Moreover, conventional conservative methods have inherent dangers, including inefficiency and the possibility of recurrence. These facts support the need to explore new conservative approaches for EC. Photodynamic therapy (PDT) is a minimally invasive treatment that can be considered for fertility-sparing. Our group recently developed novel very promising chlorins that can be used as photosensitizers in PDT. The 4,5,6,7-tetrahydropyrazolo[1,5-a] pyridine-fused chlorins and Pt (II) 4,5,6,7-tetrahydropyrazolo[1,5-a] pyridine-fused chlorin, Px1 and Px2, respectively, were used in this study. Thus, the aim of this study was to evaluate the effectiveness of Px1 and Px2 based PDT as a treatment option in EC based on new chlorins (Px-PDT) as a conservative and minimally invasive treatment to EC.

First, PDT outcome was evaluated in ECC-1 and RL95-2 endometrial cancer cell lines. For this, assays to evaluate metabolic activity, cell viability and types of cell death, cell cycle, reactive oxygen species, mitochondrial membrane potential, and photosensitizer's internalization were performed. In a second step, an *in vitro* model of cancer stem cells was used. Through the sphere-forming protocol, CSC response to PDT was evaluated using the trypan blue and Alamar Blue assays, sphere´s projection area, as well as the photosensitizer's internalization.

The main results showed both studied chlorins are active against endometrial cancer cell lines ECC-1 and RL95-2, but Px1 has shown greater PS susceptibility, showing IC50 values below 50 nM regarding photodynamic therapy. Px1 showed PDT activity against both endometrial cancer cells, with a very low cytotoxicity against these cells in the absence of light activation, which makes this chlorin a photosensitizer of choice for PDT. Moreover, in the CSC assays was observed a decrease of viability , as well as a remarkleble decrease of sphere´s projection area.

In conclusion, both Px1 and Px2 sensitizers presented effectiveness as a treatment option in EC based on new chlorins (Px-PDT), where Px1 clearly stands out. The results obtainesd in this dissertation open new avenues for the investigation of Px1 based PDT in endometrial cancer not only *in vitro* but also *in vivo*. Another future perspective is the modulation of Px chlorins for targeting CSC.

This project was hosted at the Institute of Biophysics and at the Coimbra Institute for Clinical and Biodical Research (iCBR), Faculty of Medicine, Univeristy of Coimbra, and counted with the collaborations of researchers and clinicians from the Coimbra Chemistry Center, University of Coimbra and the Coimbra Hospital and Universitary Centre, respectively.

Keywords: Cancer Stem Cells, Endometrial Cancer, Photodynamic therapy

Resumo

O cancro do endométrio (EC, do inglês Endometrial Cancer) representa cerca de 6% dos cancros no sexo feminino, sendo a doença maligna ginecológica mais frequente em países desenvolvidos. A cirurgia radical é o tratamento primário mas em mulheres jovens ou em doentes com elevado risco cirúrgico pode não ser uma opção. Além disso, métodos conservadores convencionais apresentam riscos inerentes, incluindo ineficácia e a possibilidade de recorrência. Estes factos suportam a necessidade de explorar novas abordagens conservadoras para o EC. A terapia fotodinâmica (PDT, do inglês Photodynamic Therapy) é um tratamento minimamente invasivo que pode ser considerado para a preservação da fertilidade. O nosso grupo de investigação desenvolveu recentemente umas novas clorinas muito promissoras que podem ser usadas como fotossensibilizadores em PDT. As clorinas fundidas com anel 4,5,6,7-tetra-hidropirazolo[1,5-a]piridina e as clorinas fundidas com anel 4,5,6,7-tetra-hidropirazolo[1,5-a]piridina de platina (II), Px1 e Px2, respetivamente, foram usadas neste estudo. Assim, o objetivo deste estudo foi avaliar a eficácia da PDT com base em Px1 e Px2 (Px-PDT) como uma opção terapêutica conservadora e minimamente invasiva para o EC.

Primeiramente, a resposta à PDT foi avaliada em linhas celulares do EC, ECC-1 e RL95-2. Para isso, foram realizados ensaios para avaliar a atividade metabólica, a viabilidade celular e os tipos de morte celular, o ciclo celular, as espécies reativas de oxigénio, o potencial de membrana mitocondrial e a internalização do fotossensibilizador. Numa segunda etapa, foi utilizado um modelo in vitro de células estaminais do cancro (CSC, do inglês Cancer Stem Cells). Através do protocolo de formação de esferas, a resposta das CSC à PDT foi avaliada utilizando os ensaios do Azul Tripano e do Alamar Blue, a área de projeção das esferas, assim como a internalização do fotossensibilizador.

Os resultados principais mostraram que ambas as clorinas estudadas são ativas contra as linhas celulares do EC, ECC-1 e RL95-2, mas Px1 apresentou uma maior suscetibilidade aos fotossensibilizadores, apresentando valores de IC50 inferiores a 50 nM em relação à PDT. Px1 apresentou atividade fotodinâmica contra ambas as células tumorais do endométrio, com uma citotoxicidade muito baixa contra essas células na ausência de ativação de luz, o que torna esta clorina num fotossensibilizador para PDT. Além disso, nos ensaios com CSC foi observada uma diminuição da viabilidade, assim como uma diminuição notável da área de projeção de esferas.

Em conclusão, ambos os sensibilizadores, Px1 e Px2, apresentaram eficácia como uma opção terapêutica para o EC com base nas novas clorinas, onde o Px1 claramente se destaca. Os resultados obtidos nesta dissertação abrem novos caminhos para a investigação da PDT com base em Px1 no EC não apenas *in vitro*, mas também *in vivo*. Outra perspetiva futura é a modulação das clorinas Px para terapêutica dirigida a CSC.

Este projeto foi desenvolvido no Instituto de Biofísica e no Instituto de Investigação Clínica e Biomédica de Coimbra (iCBR), da Faculdade de Medicina da Universidade de Coimbra, e contou com as colaborações de investigadores e clínicos do Centro de Química de Coimbra, da Universidade de Coimbra e do Centro Hospitalar e Universitário de Coimbra, respetivamente.

Palavras-chave: Células Estaminais do Cancro, Cancro do Endométrio, Terapia Fotodinâmica

Index

1 - Introduction

Extensive research is certainly required in a topic as essential as oncology. New approaches for detecting, diagnosing, and treating cancer are being investigated with the goal of enhancing cancer patients' quality of life during and after treatment. (National Cancer Institute, 2021).

Cancer is a condition in which cells in the body grow out of control and, in some cases, spread to other regions of the body. These cells proliferate even in absence of external growth *stimuli*, instruct blood vessels to expand toward tumours, ignoring signals that usually tell cells to cease dividing or die, in a process called programmed cell death. With a cancer projection of 19.3 million in 2020 and 28.4 million in 2040, this disease has continued to rise (National Cancer Institute, 2021; GLOBOCAN 2020).

Gynaecological cancer includes malignancies of the cervix, ovaries, endometrium, vagina, and vulva, being considered a public health problem (© International Agency for Research on Cancer-IARC 2020). The incidence of endometrial cancer (EC) varies greatly throughout the world, being more prevalent in Europe and North America than in Asia and Africa [1]. EC comprises one of the most prevalent types of cancer in women and represents about 6% of female cancers (GLOBOCAN 2020).

EC treatment includes mainly surgical therapy. In cases with reproductive desire, several strategies have been reported including surgical resection followed by progestins with improved results in terms of response, recurrence, and live birth rate [2]. In this way, the use of this conservative treatment was directly linked to a higher recurrence rate and a worse progression-free survival rate in patients over 40 years old [3]. This fact supports the need to explore new conservative treatments to EC [3].

Photodynamic treatment (PDT) comes as a possible and practicable alternative approach for EC, once PDT is a minimally invasive treatment, with selectivity for tumour tissue, that can be considered for fertility-sparing[4].

Endometrial Cancer

The endometrium is a complex and dynamic tissue, and its composition includes epithelial cells, both luminal and glandular, surrounded by stromal cells, together comprising the innermost layer of the uterus. The primary function of the uterus is the implantation of the blastocyst and support for embryo growth [5].

EC is the most frequent gynaecological malignancy in developed countries, and it is the 4th most common cancer in women, representing about 8.7% of cancers in the female sex (International Agency for Research on Cancer-IARC 2020). The American Cancer Society estimated that in 2021, about 66,570 new cases of endometrial cancer Will be diagnosed, and about 12,940 women will die from cancers of the uterine body (American Cancer Society, 2021).

Most cases of EC are diagnosed at an early stage (80% in stage I), with survival rates at 5 years > 95% [6]. Additionally, more than 90% of cases occur in women older than 50 years (International Agency for Research on Cancer-IARC 2020). The primary treatment for this group of women is surgery staging's, which encompasses issues considering childbirth, particularly before the age of 40 (International Agency for Research on Cancer-IARC 2020).

Early menarche/late menopause, unopposed oestrogen medication, and estrogen-producing tumours are all known risk factors for EC, and most patients have a documented source of excess oestrogen, defining them as risk factors for EC [7]. Risk factors are associated with a clinical profile: a high body mass index (BMI) that is deemed overweight (BMI 25–30) or obese (BMI 30), as well as other components of metabolic syndrome symptoms (e.g., hypertension, diabetes) [7]. Diabetes mellitus, particularly type II, has been identified as an independent risk factor for EC, with the potential for a significant increase in the number of cases. Infertility and nulliparity are also recognized as risk factors, as well as polycystic ovarian syndrome (PCOS), which is a common cause of infertility [7].

Bokhman, in 1983, proposed a categorization of two EC histological subtypes (Table 1). This approach was widely adopted as a standard prognosis, including the importance of adjuvant treatment that reflects the biological behaviours of cancers within each of these groups. Type I is the major group, affecting 70% of patients, and is associated with endometrial hyperplasia associated which hyperestrogenism [8]. Type II EC, on the other hand, has an aggressive clinical behaviour, more frequent in an advanced stage, as well as a higher likelihood of disease recurrence [8].

Table1: Categorization of two EC subtypes [8]

	Type I	Type 2
Phenotype	Younger age	Older age
	Obese	Nonobese
	Associated lipid and metabolic disturbances	Lack of associated lipid and metabolic disturbances
	Thickned endometrium	
Pathogenesis	Estrogen dependent	Estrogen independent
Histology	Endometrioid	Nonendometrioid
Differentiation	Well/Moderately differentiated	Poorly differentiated
Prognosis	Good	Poor
Molecular aberrations	PTEN, MSI, PI3K/AKT, KRAS	P53, Her2, P13K/AKT, KRAS

Regarding the signs and symptoms, about 90% of EC cases are manifested through abnormal uterine bleeding, as well as usually preceded by atypical endometrial hyperplasia[6].

Although the incidence of EC is increasing, the assessment of patients with early-stage cancer remains a challenge, particularly in personalized adjuvant treatments that avoid overtreatment and its associated short- and long-term toxicity [8].

Regarding the therapeutic options, EC is usually treated primarily with surgery, specifically total hysterectomy, along with bilateral salpingo-oophorectomy (BSO), as a standard [8]. European Society for Medical Oncology (ESMO) guidelines do not recommend lymphadenectomy surgery for low-risk, grade 1 or 2 diseases, it is an option for grade 3 and recommended for all stages of non-endometrioid histology [8]. Other approaches as radiotherapy, chemotherapy and hormonotherapy are fundamental for patients with of risk of recurrence in EC [6]. Besides that, the use of progestogens is widely applied as conservative treatment in patients with reproductive desire, with response rates of 75% and recurrence rates of around 40%[7].

According to The Cancer Genome Atlas Research Network (TCGA), funded by the National Cancer Institute, a molecular study of EC was performed to comprise this disease in genome and proteomics instances. It was identified an increase in progesterone receptor expression, suggesting potential responsiveness to progestin therapy.

Many strategies are emerging in this area to improve both diagnosis and therapy, including the role of surgical lymph node assessment and the selection of patients for adjuvant radio and chemotherapy approaches, as well as the use of specific markers. Another current method used as a stratification biomarker is p53, a protein that inhibits the development of cancer, and tightly regulates cell growth by promoting apoptosis[10]. Nevertheless, more research and understanding about the process of identification and mechanism of action is still required[8]. In this context, it is evident that several studies are being conducted to find new approaches, treatments, and targets for EC.

Endometrial Cancer Stem Cells: an overview

Historically, cancer research and treatments were founded on the clonal evolution theory, which argues that tumour cells develop from the successive expansion of preexisting somatic mutations. This theory[9] leaves some open questions including the evidence of clonal heterogeneity of tumours, allowing the development of drug resistance. Moreover, increasing evidence has recently led to the formulation of the so-called Cancer Stem Cells theory, which assumes that tumours, like normal tissue, are composed of cells at various stages of maturation, including CSCs [10].

These cells exhibit stem-like features, having acquired the oncogenic mutation and gaining the ability to self-renew and differentiate. This process led to the formation of the complete neoplastic cell population, as well as heterogeneity, treatment resistance, and invasiveness [10].

As illustrated in Figure 1, cancer stem cells represent a minor population of cells that are responsible for tumour initiation and maintenance, due to their proliferative potential, the capacity of self-renewal and differentiation. Moreover, they can stimulate tumour capacity of migration, invasion, and metastasis [12].

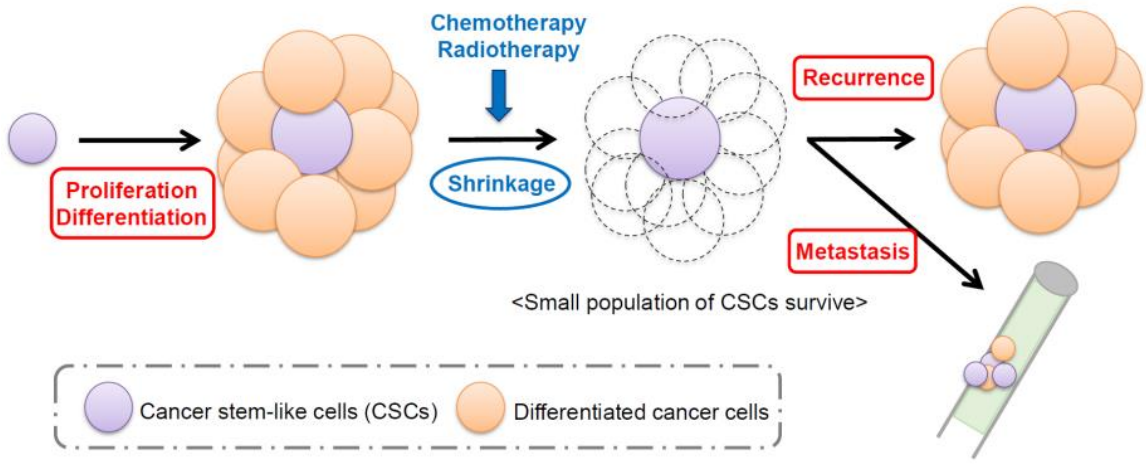

Figure 1: Mechanism of recurrence and metastasis developed from CSCs. Since their ability to self-renew and generate differentiated cell populations, CSCs are regarded to have a high tumorigenic potential. CSCs can also survive chemotherapy or radiation, which promotes recurrence and metastasis, two key reasons for poor patient outcomes. Cancer stem-like cells (CSCs) are cells that are similar to cancer stem cells. Image from Murayama et al. 2019[13].

Nevertheless, these cells are based on the establishment of resistance mechanisms and have a relationship with the development of more aggressive cancers with poor prognosis and were already identified in endometrial cancer [12 14]. So, if therapies are targeted to these cells, the cancer niche would be destroyed.

In adult tissues, stem cells (SCs) are responsible for tissue homeostasis and regeneration. Upon division, SCs can give rise to transit-amplifying (TA) cell populations, which after several divisions will finally differentiate and eventually be lost from the tissue. Also, adult SCs are activated following injuries, rapidly expand, and contribute actively to tissue repair [14].

In the cancer process, these types of cells will promote an environment that will promote the cancer cells survival. Consequently, from the CSC, may occur tumour initiation and maintenance, due to their proliferative potential, the capacity of self-renewal, differentiation, and tumour capacity of migration, invasion, and metastasis. Moreover, these cells are responsible for the establishment of resistance mechanisms and have a relationship with the development of more aggressive cancers with poor prognoses [14].

In EC, patients with relapse and advanced disease, the prognosis is still dismal, and the development of resistance is common. In this context, endometrial CSC is stem-like cells capable of self-renewal and differentiation in mature cancer cells, representing a potential field of expansion for targeting therapies [10]. The first evidence of CSC in EC,

according to Hubbard et al., came from the small populations of cells obtained from EC samples that were tumorigenic in immunocompromised mice [10].

The morphology of offspring cells was similar to a parental tumour, presenting the expression of cytokeratin, vimentin, estrogen receptor-α (ERα), and progesterone receptor (PgR), suggesting that a small population of cells can still maintain characteristics of the parental tumour and differentiate in vivo [10]. These cells play a crucial role in both the maintenance of the tumour and targeting these cells can eliminate the cancer niche. Preclinical data propose that current cancer treatment strategies lead to CSC enrichment, contributing to chemo and radiotherapy resistance [15].

Moreover, the increased expression of ATP-binding cassette (ABC) transport proteins, which are responsible for drug efflux, is one potential mechanism of chemotherapy resistance in CSC. The relative resistance of stem cells to the harmful effects of chemotherapeutic medicines is due to a higher expression of ABC transport proteins in stem cells compared to non-stem cells populations [15].

Photodynamic treatment

Photodynamic therapy (PDT) consists of treatment based on the combination of three elements that are not toxic individually: a photosensitizer (PS), visible light of a specific wavelength, and molecular oxygen. The administration of the PS and further irradiation with visible light, in a specific wavelength, leads to cell death by the generation of reactive oxygen species (ROS) in the tumour cells. PDT is indicated for the treatment of several types of cancer [16] and currently, the clinical application of PDT is well established in medical and surgical areas. It is successfully used in dermatology, urology, gastroenterology and neurosurgery [7].

PDT's dual-specificity is based on both PS accumulation in malignant tissue and targeted light delivery17. PDT has extensively researched tetrapyrrole structures such as porphyrins, chlorins, bacteriochlorin, and phthalocyanines with appropriate functionalization as photosensitizers, and several drugs have obtained clinical approval [18].

The majority of PSs applied in cancer therapy have a tetrapyrrole backbone, which is analogous to the structure of haemoglobin's protoporphyrin prosthetic group [18]. The most effective PSs comprise hydrophobic chemicals that diffuse quickly into tumour cells and settle in internal membrane components like mitochondria and endoplasmic reticulum

(ER) [18]. Many hypotheses have been presented to explain why PDT has long been recognized to have tumour-localising effects. These interpretations include the presence of leaky and tortuous tumour blood vessels, which are characteristic of the neovascularization process that occurs during tumour angiogenesis. Furthermore, when combined with the lack of lymphatic drainage in tumours, are regarded as the enhanced permeability and retention (EPR) effect [18,19].

From that, the principle of this treatment is the specific cell accumulation of the PS molecule, which has no cytotoxicity *per se*, in the tumour tissue. The followed irradiation, with monochromatic light, allows all the generation of ROS. The irradiation of the PS within the tumour results in the oxidation of intracellular oxygen and other substrates. The resulting ROS, produced in high concentrations, are cytotoxic and trigger tumour cell death [4].

Since the PS does not have cytotoxicity per se, its systemic administration does not result in unwanted effects. As an example, most therapies such as chemotherapy and radiotherapy, which eliminate tumour cells, often have severe effects on the rest of the body, which can range from tiredness and flu-like symptoms to hair loss and blood clotting problems [20]. Another known advantage of PDT is a local therapy with no long-term side effects. Also, mutations that confer resistance to radiotherapy or chemotherapy do not compromise the anticancer power of PDT [21].

Temporary skin and eye photosensitivity reactions, among the limitations of PDT, have been identified as the most significant disadvantages, and the necessity to minimize exposure to sunlight. In addition, deeply located tumours are more difficult to treat due to the low penetration of visible light into the tissues [21].

Concerning the Photobiology, illustrated in Figure 2, PDT outcome depends on several factors, including the type of PS and its concentration of administration. When a molecule absorbs light and is stimulated, it can lose energy by physical processes or contribute to chemical reactions, depending on its physical-chemical properties [22]. Besides that, the activation promoted by visible light will lead to the electronic excitation of the molecule, the PS, from its ground state to a singlet excited state.

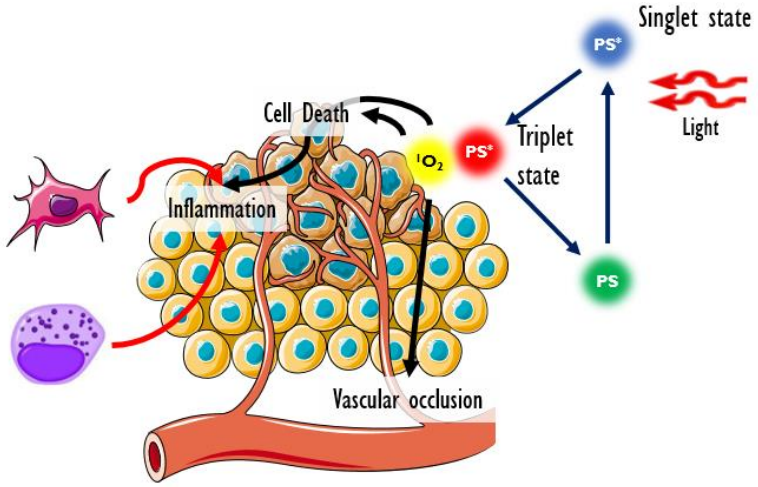

Figure 2: Schematic of photobiology PDT process in a tumour. Reactive molecular species are produced in response to light activation, causing cytotoxicity in target cells. It is represented the impact of the treatment in cellular and tissue modulation on the tumour microenvironment, resulting in tumour cell death, vascular occlusion, and inflammation. [4] Being $^1O_2$ singlet oxygen, PS photosensitizer, in green, without irradiation and in red, after irradiation.
Image from Laranjo 2014 [23]

Concerning Photobiology, PDT outcome depends on several factors including the photosensitizer (PS) (type, concentration), the light that (as the fluency, energy), the oxygen concentration, and the tumour cell type and the microenvironment. Focusing on the photosensitizer role, in the context of the tumour, the green PS is representing the one that we are going to use in the experiments (figure 2). Once excited with the light, this PS will be excited to a Singlet and Triplet state, in red (figure 2). In this stage, it has enough energy to produce ROS inside cancer cells, which will result in an unfavourable environment for its survival [4].

The formation of reactive oxygen species in high concentrations inside cells is toxic and ends up leading tumour cells to cell death. In addition, PDT can also act on the vascularization of the tumour, isolating it from the supply of oxygen and nutrients essential to its survival. Today we also know that the local inflammatory process can, in certain circumstances, have important repercussions at the level of the immune system, contributing to local and even distant tumour regression [4].

Focusing on the PS role and the Photochemistry, once excited with the visible light, the PS have pairs of electrons with opposed spins in low-energy molecular orbitals in their ground (singlet) state. The absorption of light of the right wavelength elevates an electron to a high-energy orbital while leaving its spin constant. The PS can lose its energy and revert to the ground state by producing light (fluorescence) or heat, which is a short-lived

(nanoseconds) excited singlet (S 1) state. However, the S 1 state can go through via a phenomenon is known intersystem crossing event, in which the excited electron's spin is inverted. The excited triplet (T 1) state, in red (figure 2), has an unusually long life (microseconds) due to this inversion of the electron spin [22].

Type I and Type II [22] reactions are triggered by the photobiology process of PDT therapy. The PS absorbs and transforms into a singlet when its energy levels change. The triplet state is the most important since it contains the most energy while also being the most stable, allowing it to oxidize nearby substrates [22] These two reactions occur simultaneously, and its extension between them depends on the substrate, the oxygen concentrations, the amount of available oxygen and, finally, the type of PS used. In the type I reaction, the PS reacts directly with the biomolecules in the cellular microenvironment. In biological systems, this produced radical reacts with water to produce hydrogen peroxide (H_2O_2), which can cross cell membranes and lead to direct intracellular damage. In addition to being the most reactive ROS, it has the shortest lifetime and diffusion distance [22,23].

As illustrated in figure 3, in Type II reaction, the PS transfers its energy directly to the oxygen of the ground state. This energy produces the excited state of oxygen - oxygen singlet ($1O_2$) - one of the most important ROS that can damage the cancer cells. Its useful life and, consequently, its diffusion distance, are extremely limited by its own physical and chemical characteristics. These characteristics directly influence the fact that singlet oxygen can only interact and oxidize biomolecules and structures in its short time [22.] As a result, the Type II reaction's efficiency is highly dependent on the length of the triplet state. In PDT, the singlet oxygen formed in the Type II reaction is considered the main cytotoxic species formed during the photodynamic process [23].

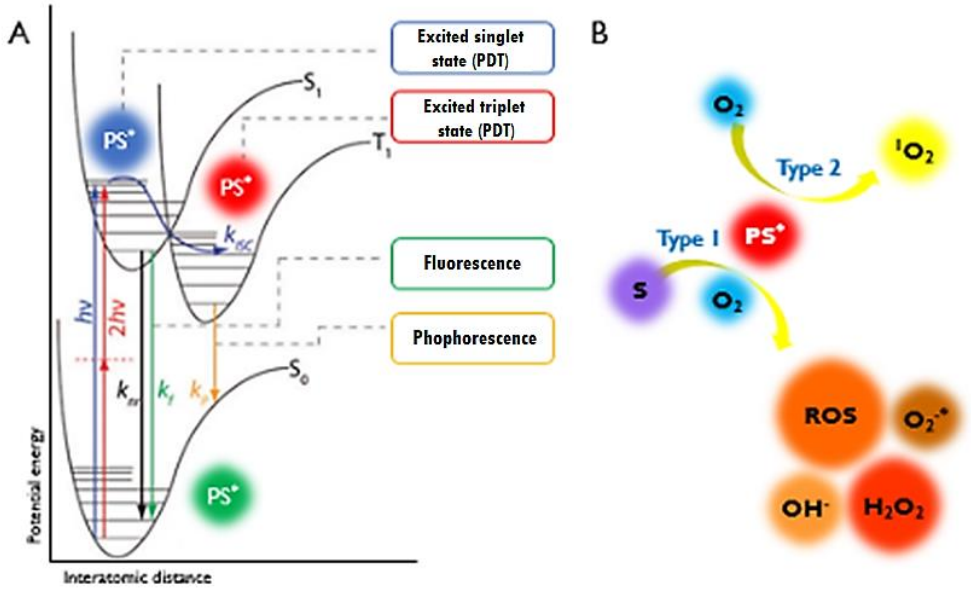

Figure 3: Type I and Type II reactions triggered by the PDT therapy. These two reactions occur simultaneously. In the type I reaction, the PS reacts directly with the biomolecules in the cellular microenvironment, leading to produced hydrogen peroxide (H_2O_2). In Type II reaction, leading to the production of the excited state of oxygen - oxygen singlet ($^1O_2$) - one of the most important ROS that can damage the cancer cells[4]. Image from Laranjo 2014.[23]

Also, PDT can act on the vascularization of the tumour (figure 2), isolating it from the supply of oxygen and nutrients essential to its survival. Currently, we also know that the local inflammatory process can, in certain circumstances, have important repercussions at the level of the immune system, contributing to local and even distant tumour regression. Pre-clinical studies describe three different and related mechanisms, which contribute to the control of tumour growth and occasional complete tumour destruction observed after PDT treatment[24]. Assuming, first, that ROS generated by PDT directly kill cancer cells at the primary site, it can happen mainly through apoptosis, necrosis and/or autophagy-related cell death. Secondly, that PDT influences endothelial cells of associated tumours vasculature, ensuring a significant decrease in blood flow and which can lead to tumour death due to starvation. Both mechanisms act on the tumour, which seems to trigger an early localized inflammatory response[24,25]. Third, a systemic response may also develop, which might be capable of preventing tumour recurrence and metastasis, in the long term[25].

Currently, there are several PSs approved for clinical use. However, to be considered ideal for clinical practice, PSs must have certain characteristics, such as being a chemically pure compound with accumulation in the tumour, providing a rapid

elimination from the body and a present a great absorption value in the 600 nm region 26, as well as their energetic states.

The 4,5,6,7-tetrahydropyrazolo[1,5-α] pyridine-fused chlorins, such as the Px1 and Px2, synthesized by our research team [4] were studied. Px1, di(hydroxymethyl)-substituted chlorin, and Px2, which can be used as a theranostic agent being a Pt-chlorin were analyzed. These compounds exhibited excellent photophysical and photochemical characteristics in addition to their great activity as a PDT agent and the absence of cytotoxicity *per se*. In fact, these chlorins *in vitro* photocytotoxicity were proved in numerous cancer types, including human melanoma, oesophageal, and bladder carcinomas.

PDT and Endometrial Neoplasms

Currently, one of the most important approaches is the maintenance of the normal life of the patients after treatments, including the cure. For this, the preservation of fertility, using a conservative treatment in younger women, should be thought and studied deeper [26].

In this context, Photodynamic Therapy (PDT) shows itself as a promising treatment for Endometrial Neoplasms, due to the easy access offered by hysteroscopy and due to providing a safe conservative option. This treatment is becoming widely accepted as an important and potential approach for cancer and some nonmalignant diseases [27].

Some studies already demonstrated the potential therapeutic role of PDT in patients with early-stage endometrial neoplasm [28,29]. Nevertheless, PDT was employed as palliative treatment to alleviate symptoms in another trial, however, the results were quite transitory. In 70.8% of endometrial malignancies, complete response was obtained, and the treatment was considered safe and successful, especially in locoregional recurrence [30]. More recently, *Choi, M. C. et al.* showed the promising result of the combined multimodal treatments, in which women were treated conservatively by hysteroscopic and laparoscopic operations. This approach was particularly important to eradicate the potentially remaining tumour by PDT and to suppress recurrence by adjuvant therapy. These studies using conventional photosensitizers supported PDT potential in this specific environment and its benefits [20], reducing the rate of metastasis and recurrence, as well as reducing secondary effects in the therapeutic setting [4].

2 - Objectives

The main aim of this research is to assess the efficacy of PDT based on novel chlorins (Px-PDT) as a potential conservative and minimally invasive therapy for EC. It was the goal of this study was to assess two novel sensitizers recently developed by the research group[31,32].

Specifically, the first objective was to evaluate the novel photosensitizers-based PDT outcome in human endometrial cancer cell lines. For this, a battery of studies including evaluation of metabolic activity, viability, types of cell death, production of reactive oxygen species, photosensitizer uptake and subcellular location were performed.

The second objective was to evaluate the novel photosensitizers-based PDT specifically in endometrial CSC. For this, as *in vitro* model of cancer stem cells was performed, allowing to study of metabolic activity, viability, projection area and photosensitizer location.

3 – Materials and Methods

The experiments were conducted in a controlled environment, in ECC-1 and RL95-2 endometrial cancer cell lines, to examine the effects of a specific experimental variable, and to discover the mechanisms of biological action without interference from other factors. This chapter is divided into two sections. In **Section I** the methods used to evaluate PDT outcome in ECC-1 and RL95-2 endometrial cancer cell lines are described. Thus, it includes assays to evaluate metabolic activity, cell viability and types of cell death, cell cycle, reactive oxygen species, mitochondrial membrane potential, and photosensitizer's internalization. In **Section II**, an *in vitro* model of CSC was used. Through the sphere-forming protocol, CSC response to PDT was evaluated using the trypan blue and Alamar Blue assays, sphere´s projection area, as well as the photosensitizer's internalization.

Section I

1. Cell culture

In this experimental work were used two endometrial cancer cell lines, RL95-2 and ECC-1, both grade 2 human type I endometrioid carcinoma cell lines, obtained from the American Type Culture Collection (ATCC). Regarding RL95-2, these cells are characteristically epithelioid and derived from moderately differentiated adenosquamous carcinoma of the endometrium31. This cell line was propagated and grown adherently with a culture medium composed of Dulbecco's modified eagle medium (DMEM, Sigma D-5648) and a blend of nutrients from Ham F12 in a 1:1 ratio (F12, Sigma N-6760), supplemented with 10% fetal bovine serum (FBS, Sigma F7524), 0.005 mg/mL insulin (Sigma I0516) and 1% antibiotic (100 U / mL penicillin and 10 µg / mL streptomycin, Sigma A5955). Regarding ECC-1, a human epithelial cell line derived from an endometrial adenocarcinoma, the Roswell Park Memorial Institute 1640 medium (RPMI-1640, Sigma, R4130) culture medium was used, supplemented with 5% FBS, 400 mM pyruvate sodium (Gibco, 11360) and 1% antibiotic.

For these studies, it was necessary to detach the cells and prepare cell suspensions. Cell cultures were washed with phosphate-buffered saline solution (PBS), a solution

consisting of sodium chloride 137 nM (NaCl, JMGS, 037040005002212), potassium chloride 2.7 mM (KCl, Sigma, P9333), sodium dihydrogen phosphate 10 mM (NaH2PO4, Merck, 6580.0500), potassium dihydrogen phosphate 1.8 mM (KH2PO4, Sigma, P0662), and ethylenediaminetetraacetic acid 5mM (EDTA, VWR - M101), with a pH of 7.4. Then, cells were detached through incubation with 0.25% trypsin-EDTA (Sigma, T4049), for about 5 minutes at 37°C. Cells were suspended in the appropriate cell culture medium to inactivate trypsin.

To determine the cell concentration, an aliquot of each suspension was stained with trypan blue and placed on a hemocytometer in an inverted optical microscope (Nikon Eclipse TS 100) at 100x magnification. This method of exclusion using trypan blue allows cells to be observed and counted under a light microscope while the dead blue cells were excluded from counting. The number of cells counted in the hemocytometer allows us to infer the concentration of a cell suspension.

2. Photodynamic Therapy

Photodynamic therapy (PDT) consists of treatment based on the combination of a photosensitizer (PS) and visible light of a specific wavelength32. For each experiment, EC cell lines were plated and kept in an incubator overnight to make sure that cells were attached. The formulation of the photosensitizers consisted of a solution of 1 mg/mL of dimethyl sulfoxide (DMSO, Fisher Chemical, 200-664-3) with the desired concentrations achieved by serial dilution. Photosensitizers were administered into cells for 24 hours in several concentrations from 1 nM to 10 µM. Controls were included on every plate, as untreated cell cultures and cultures treated with the vehicle of administration of the photosensitizers (DMSO) at a concentration of 1%[33].

Cells were washed with PBS to guarantee the remotion of non-internalized photosensitizers, and a new drug-free medium was added. Each plate was then irradiated to activate the photosensitizers with a fluence rate of 7.5 mW/cm^2 until a total of 10 J was reached using a light source equipped with a red filter[16]. All assays were performed 24 hours after treatment.

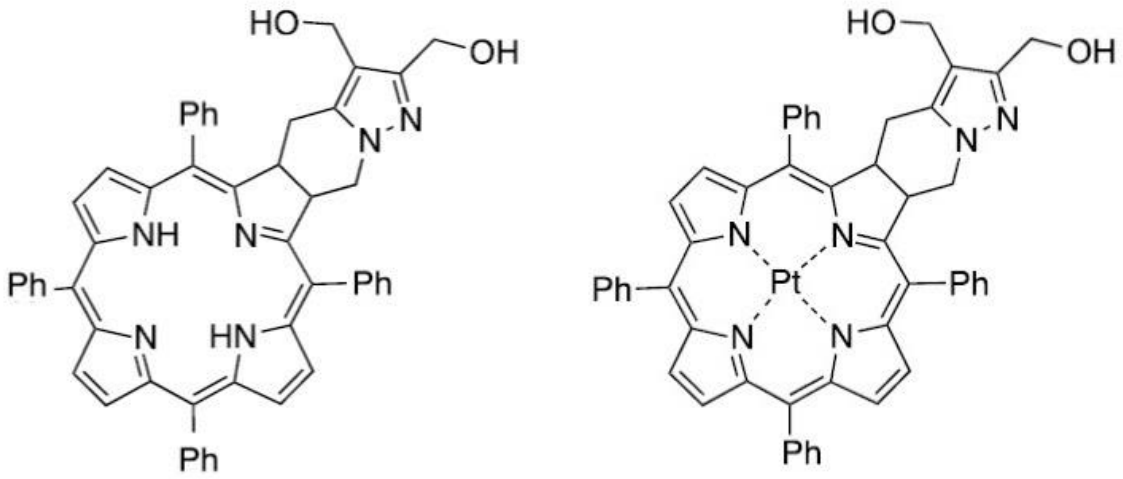

Figure 4: 4,5,6,7-tetrahydropyrazolo[1,5-α] pyridine-fused chlorin and Pt (II) 4,5,6,7-tetrahydropyrazolo[1,5-a] pyridine-fused chlorin, Px1 and Px2, used in this research, respectively4,26.

3. Photocytotoxicity

MTT is a yellowish solution of a water-soluble tetrazolium salt, 3-(4,5-dimethylthiazolyl)2,5-diphenyltetrazolium bromide. This salt is incorporated by cells and reduced, primarily by mitochondrial enzymes, to generate dark blue formazan crystals. Cells' capacity to reduce MTT suggests mitochondrial integrity and activity, which can be regarded as an indicator of metabolism activity and, as a result, viability[34].

After photodynamic treatment, metabolic activity and photocytotoxicity analysis were performed in order to obtain a dose-response curve and the respective IC_{50} of each photosensitizer.

After cell cultures were submitted to PDT, as described, the medium was removed, and the cells were washed with PBS. Then, 200 μL of an MTT solution (Sigma) at 0.5 mg/mL and pH 7.4 was added to each well, and cells were incubated overnight in the dark at 37°C in 5% CO_2. After this time, 200 μL of isopropanol (Sigma) at 0.04 M was added and the plates were agitated to dissolve the purple formazan crystals. Absorbance values were measured at 570 and 620 nm in an ELISA The results were expressed as a percentage of the metabolic activity of cultures submitted to PDT concerning the cultures treated with the photosensitizer administration vehicle.

Moreover, cell cultures were submitted to PDT, as described, but the light irradiation step was omitted. The MTT assay was performed as described above, as a means to evaluate photosensitizers cytotoxicity.

4. Photosensitizer internalization

For this study, ECC-1 and RL95-2 cell suspensions at $1.6x10^5$ and $2x10^5$ cells/ml, respectively, were plated in 24-well plates under sterilized coverslips. After cell adhesion, endometrial cell cultures were incubated with 500 nM Px1 for 24 hours.

Posteriorly, cell cultures were washed twice with PBS to remove Px1 that has not been internalized by the cells, and cells were fixed with 4% paraformaldehyde for 10 minutes in the dark at 37°C. Then, nucleus labelling was performed by incubation with 5 mg/ml DAPI (4',6-diamidino-2-phenyLindole, dihydrochloride, Invitrogen™, D1306, USA) for 15 minutes in the dark at 37°C. After incubation with the probe, cell cultures were washed with PBS, the coverslips were mounted on slides with ProLong™ Gold Antifade Mountant with DAPI (Invitrogen™, P36931, USA) and were observed under the microscope. All images were acquired with a magnification of 400x through Carl Zeiss MicroImaging LSM 710 confocal microscopy system.

5. Photosensitizer uptake

In order to quantify the photosensitizers' uptake, a calibration curve and fluorescence spectroscopy were performed. Intracellular concentration was calculated using a calibration curve derived from the fluorescence intensity of a serial dilution in DMSO. Thus, 200 µL of 10 µM DMSO was added to a 96-well plate (SPL Life Sciences, 30096), and successive dilutions were performed until the detection limit of the fluorescence spectrometer was reached (EnSpire® Multimode Plate Reader, PerkinElmer®).

$1x10^5$ cells/mL were plated and incubated through 4, 8, and 24 hours with 500 nM. Washing with PBS and scrapping process were made and, to ensure full detach and cell rupture, 100 µL of DMSO was added, and the remaining suspension was centrifuged at 2500xg. The samples fluorescence intensity was analyzed in comparison to the calibration curve, as represented in Figure 5.

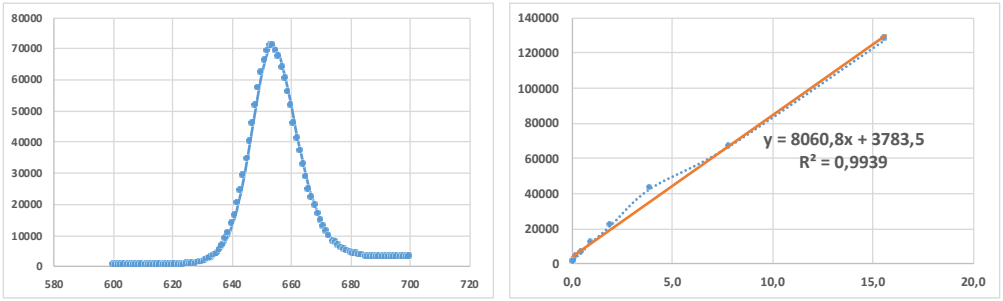

Figure 5: Uptake studies. On the left, there is an example of a fluorescence spectrum of Px1 used to obtain the calibration curves on the right side. The calibration curve was obtained through a linear fitting. The measurement of fluorescence intensity was performed considering the maximum absorption at 410 nm and the fluorescence emission peak at 645 nm.

6. Viability and cell death

One of the characteristics that distinguish live cells from dead cells is the loss of transport function or structural integrity of the plasma membrane. Flow cytometry frequently employs the PI exclusion test. It is possible to differentiate living cells from dead cells after incubation with IP[4]. Plasma membrane phospholipids are distributed asymmetrically between membrane regions in live cells. This asymmetry dissolves as apoptosis begins, and phosphatidylserine, which is typically located in the membrane's innermost layer, translocate to the luminal surface.

The protein annexin V (AnV) binds to anionic phospholipids (such as phosphatidylserine) with high affinity and is applied as a flow cytometry marker of cells undergoing apoptosis when attached to a fluorochrome (FITC, fluorescein isothiocyanate). It can distinguish between living cells, cells in early apoptosis, and cells in late apoptosis/necrosis and necrosis, by staining cells with AnV-FITC and IP. When both probes get a negative label, the detected cells correspond to living cells. If the AnV-FITC probe dying is positive but the IP is negative, the cells are in the early stages of apoptosis. If both probes are positive, the cells are in late apoptosis or necrosis, and the integrity of the plasma membrane has been compromised. Finally, if the cells are negative for AnV-FITC but positive for IP, they are in necrosis[17].

Cell cultures were submitted to PDT using a concentration of 100 nM of Px1 and Px2. ECC-1 and RL95-2 cell cultures were centrifuged at 1000 xg, and the pellet was

incubated for 15 minutes in the dark and at room temperature with 100 µL of binding buffer (0.01 M Hepes [Sigma, H7523], 0.14 M NaCl [Sigma, S7653], and 0.25 mM CaCl2 [Sigma, C4901]), 2.5 µL of AnV-APC (Immunostep AnXVF KIT Immunotech), and 1µL of IP (KIT Immuno). After incubation, 400 µL of PBS were added and analyzed. The fraction of live cells, cells in apoptosis, late apoptosis/necrosis, and necrosis were obtained as a percentage.

7. Cell cycle

Flow cytometry was used to assess the effects of the compounds on cell cycle progression (G0/G1 phase, G2/M phase, and S phase) after treatment with 100 nM of both Px1 and Px2. Since PI intercalates with both DNA and RNA bases, this experiment requires the use of RNase to generate just DNA-specific labelling 35.

As a result, cells in the S phase will contain more DNA than cells in the G1 phase. They will absorb proportionally more dye and glow brighter until their DNA content has doubled. The G2 cells will be almost twice as luminous as the G1 ones.

$1x10^6$ cells of each EC cell line were detached from the plates and centrifuged 1000xg for 5 minutes for each experiment. To fix the cells, 200 µL of 70% ethanol was added to the samples in the vortex and then incubated in the dark at 4°C for 30 minutes. Following the incubation period, the samples were centrifuged at 2500 rpm for 5 minutes, washed with 2 mL PBS, and 200 µL of PI/RNase solution (Immunostep, PI/RNase) was added to the resultant pellet and incubated for 15 minutes at room temperature in the dark. The experiment was carried out using a FACSCalibur flow cytometer (Becton Dickinson) with excitation and emission wavelengths of 488 and 640 nm, respectively. The proportion of cells in each subpopulation sub-G0/G1, G0/G1, S, and G2/M was obtained.

8. Mitochondrial membrane potential

The collapse of mitochondrial membrane potential ($\Delta\Psi$) is one of the early stages, if not the cause, of apoptosis36,37. The fluorescent dye JC-1 (5,5′,6,6′-tetrachloro-1,1′,3,3′-tetraethyl-imidacarbocyanine iodide) can be used to test it. JC-1 is a lipophilic and cationic dye that enters the mitochondria as monomers (M), which organize into aggregates (A) under mitochondrial polarization conditions and generate fluorescence in the red zone. JC-1 is excluded from the mitochondria when the $\Delta\Psi m$ decreases, and it is disseminated throughout the cytoplasm as monomers that produce fluorescence in the

green zone. Regardless of mitochondrial density, the ratio between red and green fluorescence (A/M) provides an estimate of the $\Delta\Psi$ [38].

For each experiment, $1x10^6$ cells were detached from plates, centrifuged at 2500 rpm for 5 minutes, and then resuspended in 1 mL PBS. The samples were then centrifuged under the same circumstances and incubated for 15 minutes at 37°C in 5% CO_2 with JC-1 (Sigma, T4069) at a concentration of 5 mg/mL. After that, each sample was centrifuged for 5 minutes with 2 mL of PBS added. Finally, 400 mL of PBS was added, and the monomers and aggregates were detected in a FACSCalibur cytometer using excitation wavelengths of 530 nm and 590 nm, respectively. The results are given as the ratio variation of monomer/aggregate fluorescence intensity (M/A), normalized to the control.

9. Singlet oxygen and hydroxyl radical production

The presence of singlet oxygen and hydroxyl radical scavengers (sodium Azide and D-mannitol, respectively) was used to assess the relative contribution of these species for Px-PDT, as previously described by Obata and colleagues[39].

The ECC-1 and RL95-2 cells were plated, and 100 nM of both Px1 and Px2 were administered under the same conditions as before. After 24 hours of incubation, cells were washed with PBS and media containing ROS inhibitors such as NaN_3 (5 mM, Sigma 71290) or D-mannitol (40 mM, Sigma M4125) were added. The cell cultures were incubated for 2 hours at 37°C with 5% CO_2 before being irradiated. Following irradiation, the cell cultures were incubated for 30 minutes at 37°C with 5% CO_2, before being administered new free-ROS inhibitors media. The MTT test was performed as previously described.

10. Peroxides production

The conversion of 2'-7'-dichlorodihydrofluorescein (DCFH2) to the fluorescent molecule 2'-7'-dichlorofluorescein (DCF) is a relatively specific indication of H_2O_2 production. DCFH2-DA, the diacetate form of DCFH, is absorbed by cells, whereas DCFH-DA is metabolized by cells to produce DCFH, which is then retained intracellularly.

DCFH is oxidized to DCF in the presence of hydrogen peroxide, producing fluorescence at a wavelength of 522 nm following excitation with a wavelength of 490 nm.

The concentration of intracellular peroxides, namely hydrogen peroxide, is proportional to fluorescence[4] and was quantified as previously described[40].

Cell suspensions were centrifuged at 2500 rpm for 5 minutes after being washed with PBS. The pellet was suspended in 1 mL PBS and incubated in the dark at 37°C for 45 minutes with 5 μM DCFH2-DA (Molecular probes, Invitrogen). The suspension was rinsed in PBS, centrifuged for 5 minutes at 2500 rpm, and then, suspended in a buffer. Fluorescence was read (EnSpire® Multimode Plate Reader, PerkinElmer®) under an excitation wavelength of 494 nm and an emission wavelength of 519 nm.

11. Superoxide's production

The DHE probe was used to analyze the intracellular production of superoxide radicals. Since this chemical is lipophilic, it may easily penetrate the cell membrane into the intracellular compartment, where it is converted to ethidium by the superoxide radical. Ethidium is a red fluorescent chemical that can incorporate itself into DNA, allowing it to remain inside the cell.

Cell suspensions were centrifuged at 2500 rpm for 5 minutes after being washed with PBS. After that, the pellet was suspended in 1 mL of PBS with 5 μL of DHE (Sigma Aldrich, D7008), to obtain a final concentration of 5 μM, and incubated at 37°C for 15 minutes. The suspension was rinsed in PBS, centrifuged for 5 minutes at 2500 rpm, and then, suspended in a buffer. The excitation wavelength of 620 nm was used to read the fluorescence in the EnSpire® Multimode Plate Reader, PerkinElmer®.

Section 2

1. Sphere-forming protocol

The tumour-spheres consist of a three-dimensional model for the study and expansion of CSC and have a spherical and solid structure that develops from the proliferation of a single progenitor/stem cancer cell. These cells grow in a medium without FBS, in non-adherent conditions to enrich the populations of CSC, like the ones with the capacity to survive and to proliferate in this environment[37,38].

In this work, the sphere-formation protocol used was adapted from protocols described in previous works[2,3,39.] Suspension cell culture flasks and plates (Sarstedt, 83.3920.500/Sarstedt, 83.1813.500, Corning Incorporated Life Sciences, New York, USA) were coated with poly (2- hydroxyethyl-methacrylate) (Sigma-Aldrich, Saint Louis, USA, P3932) to make sure that cells will not be attached5.

ECC-1 cell line was cultured with DMEM-F12 supplemented with 100 mM putrescine (Sigma, P5780, Sigma-Aldrich, Saint Louis, USA), 1% insulin-transferrin-selenium-A (Gibco, 51300-044, Life Technologies Europe, Grand Island, USA), and 1% methylcellulose (Sigma-Aldrich, Saint Louis, USA). To make sure these cells would develop undifferentiated profiles during the protocol, epidermal growth factor (EGF, Sigma, E9644, Sigma-Aldrich, Saint Louis, USA) and fibroblast growth factor (bFGF, Sigma F0291, Sigma-Aldrich, Saint Louis, USA) were supplemented every two days at a concentration of 10 ng/mL[5,6].

2. Photosensitizer internalization in CSC

Regarding endometrial CSC, the sphere-forming protocol was performed as previously described. After that, spheres obtained from the ECC-1 cell line (ECC-1 ES1) were plated in a 24-well plate and incubated with 500 nM Px1 for 24 hours. Then, endometrial CSC was centrifuged and washed twice with PBS and incubated with 5 mg/ml DAPI for 15 minutes in the dark at 37°C. After this period, CSC was washed with PBS, fixed with 4% paraformaldehyde for 30 minutes in the dark at 37°C, washed with PBS and mounted on slides and Z-stack images acquired in the confocal microscope.

3. CSC viability

In order to analyze the spheres viability submitted to PDT, the Trypan Blue assay was used. In this assay, ECC-1 ES1 were treated with a range of concentrations between 100 nM and 1 μM, for 4 and 24 hours of incubation. After 24 hours of irradiation, cell trypsinization was performed to analyze spheres-obtained single cells.

A known volume of the cell suspension was diluted in an equal volume of 0.4% trypan blue and counted in an inverted microscope (Motic AE31), with a 100x magnification. Thus, the number of living and dead cells was calculated using a

hemocytometer. Cell viability for each studied condition has been obtained by the relation between the number of living cells and the total cell number.

4. CSC metabolic activity

The cytotoxic impact of PDT on ECC-1 ES1 was determined using the Alamar Blue® assay. This assay uses resazurin, an oxidation-reduction reaction indicator dye, to measure cellular metabolic activity. The transition from the oxidized to the reduced state is marked by a shift in colour from dark blue to pink, which may be measured using spectrophotometry.

After the sphere-forming protocol, ECC-1 ES1 were distributed into 48-well plates (Costar, 3548). 24 hours after photodynamic treatment with both photosensitizers (from 100 nM to 1 µM), the Alamar Blue® reagent was applied to each well at a concentration of 10% and incubated in the dark at 37°C until there was a noticeable change in the colour of the dye, and the absorbance was measured at 570 nm and 600 nm to determine cellular metabolic activity.

The results were expressed as a percentage concerning the control, considering each studied condition, and measured with an EnSpire® Multimode Plate Reader, PerkinElmer®.

5. Sphere's projection area

For the sphere-forming protocol, ECC-1 cells were distributed at a concentration of $1x10^6$ cells in suspension culture flasks, previously coated with polyhema, as previously referred. Obtained ECC-1 ES1 were plated in 48-well plates and incubated with Px1 and Px2 (from 100 nM to 1 µM) for 24 hours. After that, plates were irradiated as previously described. After 24 hours, 5 random plans of each well of the studied conditions was photographed with a Moticam 1080 camera (Nikon, Eclipse TS 100, Japan) at 100x magnification, using a Motic Images Plus 3.0 software. ImageJ software was used to analyze the obtained images, by drawing the areas of interest corresponding to the spheres.

All groups of cells of spherical morphology with a diameter superior to 40 µm are considered in this experiment, Data were expressed, in pixels, corresponding to the total area of the spheres of each plan.

6. Statistical analysis

The GraphPad Program® software was used to perform the statistical analysis of the quantitative data obtained through this chapter. In the following chapters, mean standard errors were used to express the outcomes of the quantitative variables discussed throughout the paper.

The results of the metabolic activity were adjusted to a sigmoidal model of dose-response and the IC50 values were derived through the mathematical model.

The normality of the distribution of quantitative variables was assessed using the Shapiro-Wilk test.

The comparison of metabolic activity and production of reactive oxygen species of the cell cultures submitted to treatment with that of the control cell cultures was performed with the t-student test for one sample, and the sample value of each group was compared with the normalization value. In the case of the experiments where reactive oxygen inhibitors were used the experimental values were compared with the metabolic activity derived from the dose-response curves (considering the concentration of the tested photosensitizer of 100nM).

After establishing the normal distribution and homogeneity of variances, the ANOVA test was used to compare cell populations in investigations of types of cell death cell cycle, mitochondrial membrane potential, oxidative stress, and the sphere projection area. The Kruskal-Wallis test was employed in circumstances where normality was not verified. Multiple comparisons were corrected with Dunn or Dunnet test as applicable.

4 - Results

Section 1

1. Photocytotoxicity and cytotoxicity

After 24 hours of photodynamic treatment, the MTT results for both PS were adjusted to a sigmoid dose-response model. The dose-response curves of the ECC-1 and RL95-2 cell lines are shown in Figures 6, respectively. The mean point, corresponding to the IC_{50} value, was determined from the equation of each curve, along with the respective 95% confidence intervals and R^2 of the curves, according to the following table.

Table 2: IC50 values of both photosensitizers in endometrial adenocarcinoma cell lines ECC-1 and RL95-2, 24 hours after photodynamic treatment.

PS	**ECC-1**				**RL95-2**		
	IC_{50} (nM)	$CI_{95\%}$	R^2		IC_{50} (nM)	$CI_{95\%}$	R^2
Px1	28,63	26,35 to 30,99	0,9485		45,52	34,67 to 65,07	0,8973
Px2	53,46	48,64 to 59,02	0,9577		95,27	49,75 to 197,5	0,8439

After incubation with the PS, the obtained IC50 values were 28.63 and 45.52 nM for Px1, and 53.46 and 95.27 nM for Px2, regarding ECC-1 and RL95-2 cells, respectively.

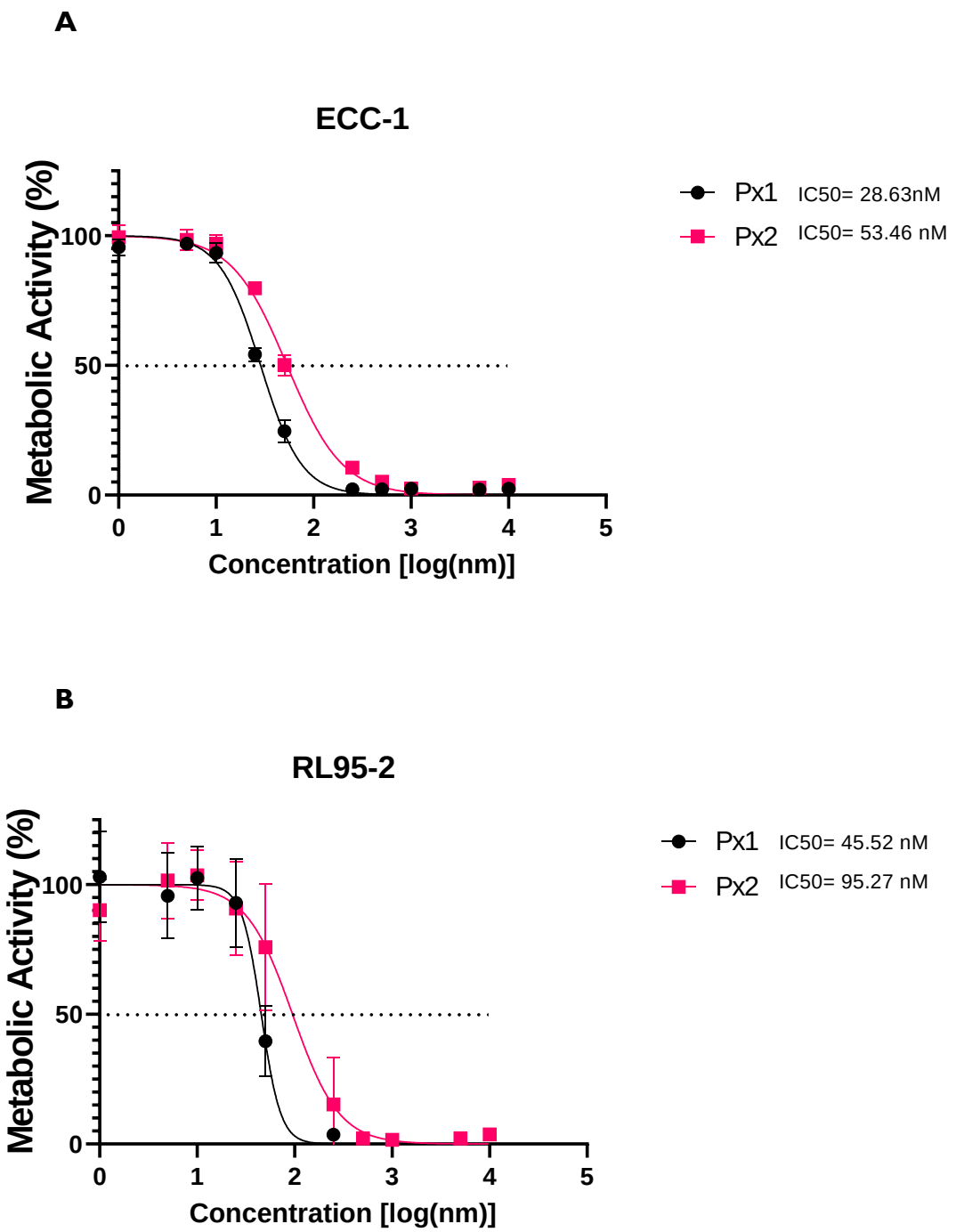

Figure 6: Dose-response curves for Px1 and Px2 based PDT for (A) ECC-1 cell line, and (B) RL95-2 cell line. This study PDT was performed using the photosensitizer in a range of concentrations, a drug-light interval of 24 hours and irradiation with 10J. Results are presented as mean ± standard error of the mean (SEM) of at least six independent trials

The metabolic activity of cell cultures that were not exposed to irradiation was also analyzed, as shown in Figure 7. The metabolic activity levels in ECC-1 and RL95-2 cell lines

for the three highest tested concentrations (10, 5 and 2.5 μM) of each PS showed none of the chemicals was cytotoxic.

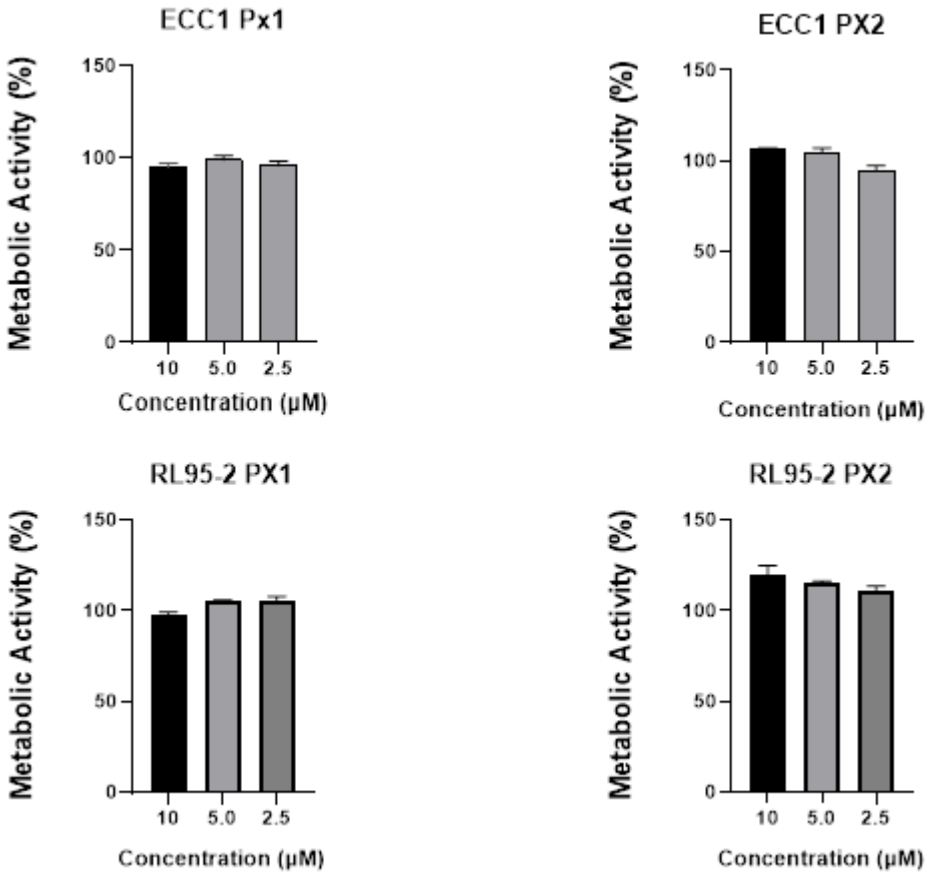

Figure 7: Metabolic activity of ECC1 and RL95-2 cell lines incubated with Px1 and Px2. In these experiments, PDT was not completed as the irradiation step was omitted. Results are presented as mean ± SEM of at least six trials. Statistical analysis: non-significant (ns).

2. Px1 internalization and uptake

Through a confocal microscopy experiment, it was possible to observe that the photosensitizer Px1 was internalized by cell lines ECC-1 and RL95-2, as illustrated in the following Figure 8. The images show the photosensitizer accumulates in the cytoplasm, but it does not seem to surpass the nuclear envelop as there is no nuclear co-localization.

Regarding cell uptake quantification of Px1, it was only possible to conduct one experiment, therefore low certainty may be attributed to such results. Nevertheless, for the ECC-1 cell line, an uptake of 1.4 nM, 14.4 nM and 41.8 nM was calculated for 4, 8 and 24 hours of incubation. Regarding RL95-2 cell lines, lower values were obtained only of 0.9nM, 6.3nM and 0.6 nM for the same timepoints.

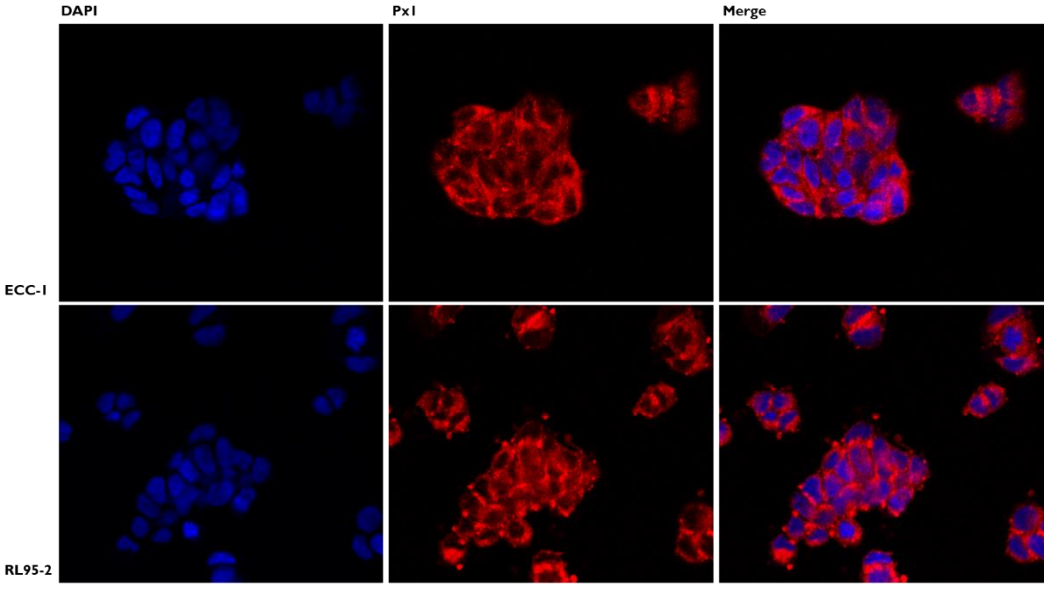

Figure 8: Confocal microscopy images representative of the subcellular location of the Px1 photosensitizer. Images were taken after 24 hours of incubation with 500 nM Px1. The left column shows the location of the nuclei in blue; the central column shows the distribution of the photosensitizer in red and the column on the right represents the overlap of each pair of images. ECC-1 endometrial adenocarcinoma cells are shown above, and RL95-2 endometrial adenocarcinoma cells are shown below. Images were obtained with a magnification of 400x.

3. Px-PDT-induced types of cell death

Figure 9 describes the cell populations identified after Px-PDT. The cell viability in control ECC-1 cell line samples was 88.9%, whereas after being treated with Px1-PDT a remarkable decrease is observed, reaching 38.36±5.78% ($p<0.0001$). Regarding late apoptosis, was observed a significant increase in Px1-PDT comparing to control from 8,450±0.2134% to 23.00±3.143% ($p<0,0001$). Also, regarding necrosis, was observed a significant increase in Px1-PDT comparing to control from 3.5±0.7032% to 35.45±6.91% ($p<0.0003$). Px1-PDT outcome was also significatively superior to Px2-PDT where the number of viable cells was 35.45±7.490 to 4.286±0.96 ($p<0,0018$). No significant differences were observed between Px2-PDT and control cultures.

The cell viability in the control RL95-2 cell line, corresponded 79.9±3.4%. Concerning PDT-Px1, it was observed a decrease to 51.20±5.2% with statistical significance ($p<0.001$) in relation to the control samples. PDT-Px1 mainly induced apoptosis in this cell line by 29.20±4.7% ($p<0.01$), but also late apoptosis by 8.0±1.3

(p<0.01), and necrosis by 11.40±1.92 (p<0.001). After being treated with Px2-PDT a moderate increase in necrosis was noticed, reaching 10.25±3.07% (p<0.05).

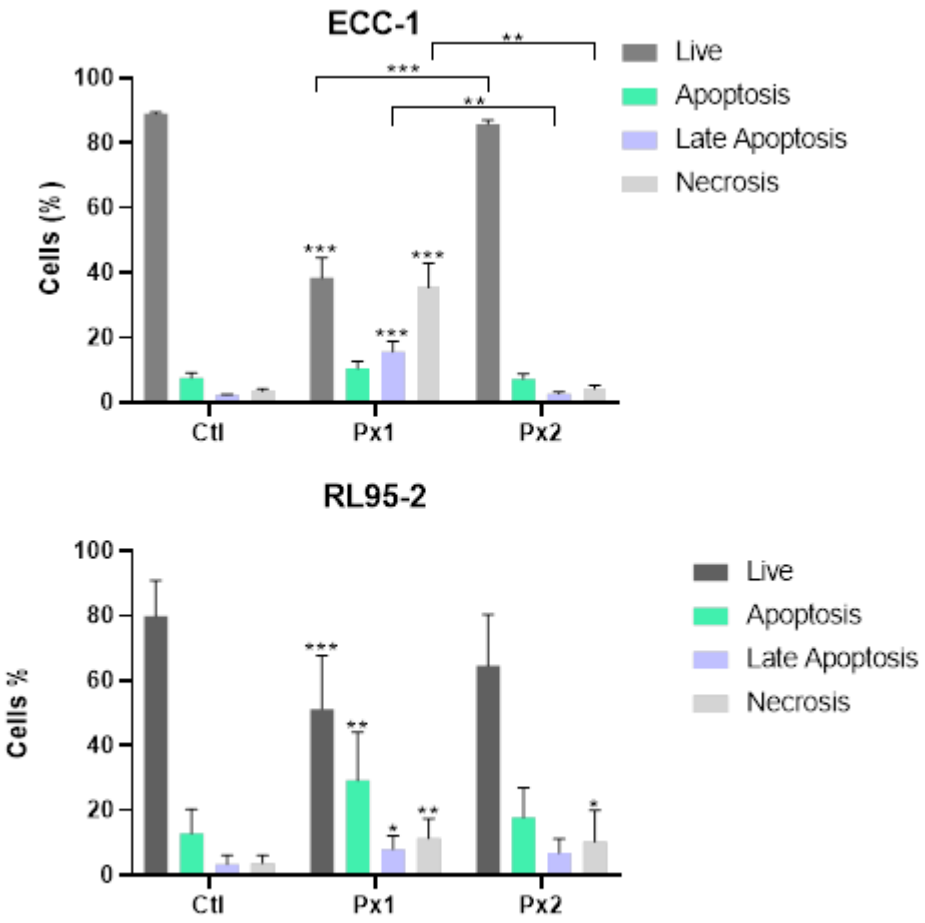

Figure 9. ECC-1 and RL95-2 cell lines viability and Px-PDT-induced types of cell death. This study PDT was performed using the photosensitizer in a concentration of 100nM, a drug-light interval of 24 hours and irradiation with 10J. The percentages of viable cells (V), early apoptosis (A), late apoptosis/necrosis (A/N), and necrosis (N) are represented. The results represent the mean and SEM of at least four independent assays. Statistically significant differences are represented with * for p<0.05, ** for p<0.001 and *** for p<0.0001.

4. Cell Cycle Analysis

The cell cycle analysis revealed important retention in the G0/G1 phase in ECC-1 treated with PDT- Px1 ($p<0.05$) in comparison to the control cultures, as shown in Figure 10. On the other hand, the S phase showed a remarkable decrease in Px1-PDT compared to control cells, reaching 38.5%±4.6% ($p<0.05$).

The percentage of RL95-2 cells in the sub-G0 stage treated with Px1-PDT was 8.83%. Despite a tendency to the retention of cells in the G0/G1 phase no significant alterations were observed regarding control that presented 60.5±0.56%. However, the consequent decrease in the S phase reached 22.5%±2.96% ($p<0,05$).

A similar distribution of cell cycle was observed after Px2-PDT. In this case, G0/G1 stage significant increase reaching 67.50± 2.30% ($p<0.05$) compared to control cells.

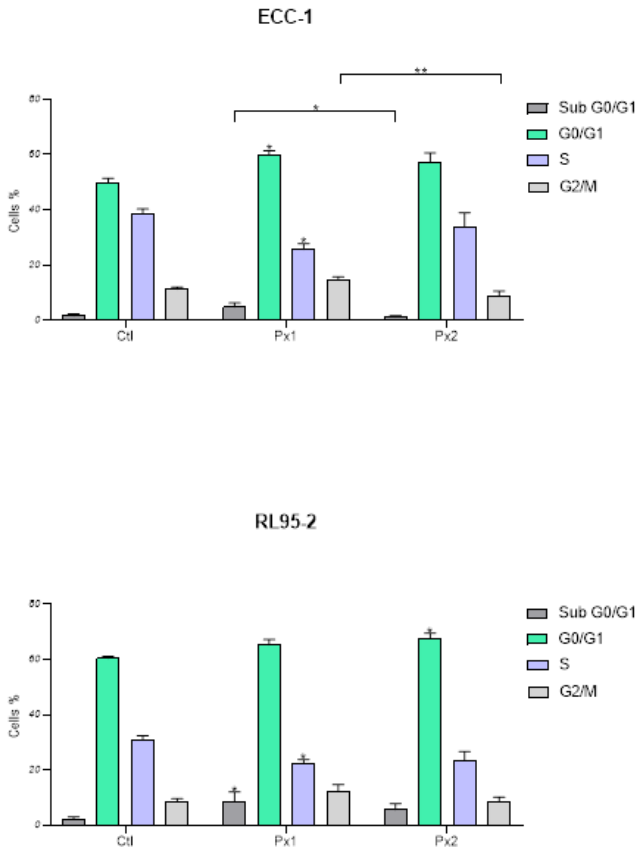

Figure 10 - ECC-1 and RL95-2 cell lines cell cycle after Px-PDT. This study PDT was performed using the photosensitizer in a concentration of 100nM, a drug-light interval of 24 hours and irradiation with 10J. The results are presented as the percentage (%) of cells in each of the phases of the cell cycle. The results represent the mean and SEM of at least three independent assays. Statistically significant differences are represented with * for $p<0.05$, ** for $p<0.001$ and *** for $p<0.0001$.

5. Mitochondria membrane potential

M/A ratio, presented in Figure 11, is inversely proportional to the mitochondrial membrane potential. Px1-PDT led to a significant loss of mitochondrial membrane potential both in ECC1 ($p<0.0001$) and in RL95-5 cells ($p<0.05$). However, no significant changes were observed when cells were submitted to PDT based on Px2.

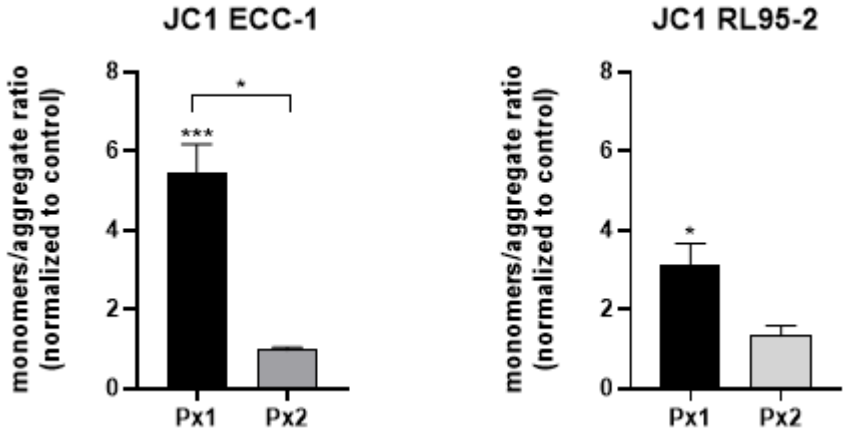

Figure 11: Mitochondrial membrane potential of PDT-treated ECC-1 and RL95-2 cell line cells. This study PDT was performed using the photosensitizer in a concentration of 100nM, a drug-light interval of 24 hours and irradiation with 10J. For each condition, the results represent the monomer/aggregate ratio (M/A). According to the potential of the mitochondrial membrane, the JC-1 probe coexists in monomeric or aggregated form; an increase in the M/A ratio suggests a decrease in mitochondrial membrane potential. The mean and SEM of eight trials are represented in the results. Statistically significant differences are represented with * for $p<0.05$, ** for $p<0.001$ and *** for $p<0.0001$-

6. Reactive oxygen species

As observed in Figure 12, Px-PDT seems to induce a reduction of peroxides in RL95-2 relative to control ($p<0.01$) while no alterations were seen in the ECC-1 cell line.

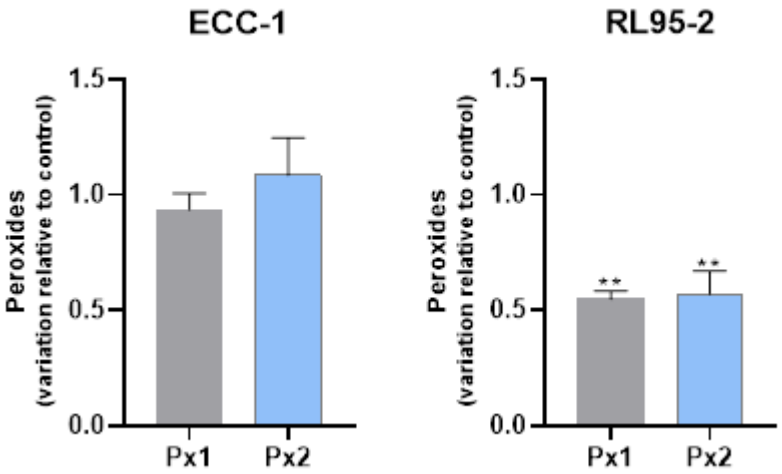

Figure12 - Peroxide production on ECC-1 and RL95-2 cells submitted to Px1 and Px2 based PDT. This study PDT was performed using the photosensitizer in a concentration of 100nM, a drug-light interval of 24 hours and irradiation with 10J. The results are shown as the variation regarding the control cell cultures. The graph shows the average and SEM of at least four different assays. Statistically significant differences are represented with * for $p<0.05$, ** for $p<0.001$ and *** for $p<0.0001$

The production of superoxide anion is represented in Figure 13. Regarding superoxide anion production by ECC-1 cells, there is a trend for the increase when submitted to Px1, although not statistically significant. No further alterations were found.

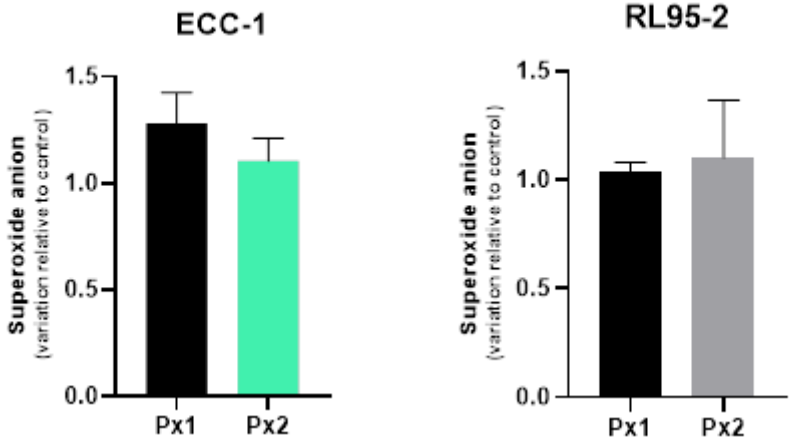

Figure 13 - Superoxide production on ECC-1 and RL95-2 cells submitted to Px1 and Px2 based PDT. This study PDT was performed using the photosensitizer in a concentration of 100nM, a drug-light interval of 24 hours and irradiation with 10J. The results are shown as the variation regarding control cell culture. The graph shows the average and SEM of at least four different assays. Statistically significant differences are represented with * for $p<0.05$, ** for $p<0.001$ and *** for $p<0.0001$.

As described, the preponderance of singlet oxygen and superoxide anion was evaluated indirectly by the use of scavengers of these species, namely, sodium azide and d-mannitol, respectively. Figure 14 shows the action of these inhibitors in Px-PDT.

Both inhibitors significantly reduced PDT's photocytotoxicity with both photosensitizers, demonstrating that singlet oxygen and superoxide anion production is crucial for photodynamic activity with these photosensitizers.

Regarding ECC-1 cells, it was observed an increased metabolic activity from 6,95% to 49.61% ($p<0.0001$) and 77.04% ($p<0.0001$) when singlet oxygen and superoxide anion were inhibited in Px1-PDT, respectively. In the case of Px2-PDT, the metabolic activity increased from 27,69% to 73.11% ($p<0.0001$) and 83.08% ($p<0.0001$) concerning respective singlet oxygen and superoxide anion inhibition.

Regarding RL95-2 cells, it was observed an increased metabolic activity from 3,14% to 65.61% ($p<0.0001$) and 88.86% ($p<0.0001$) when singlet oxygen and superoxide anion were inhibited in Px1-PDT, respectively. In the case of Px2-PDT, the metabolic activity increased from 47,79% to 70.74% ($p<0.0001$) and 72.59% ($p<0.0001$) concerning respective singlet oxygen and superoxide anion inhibition.

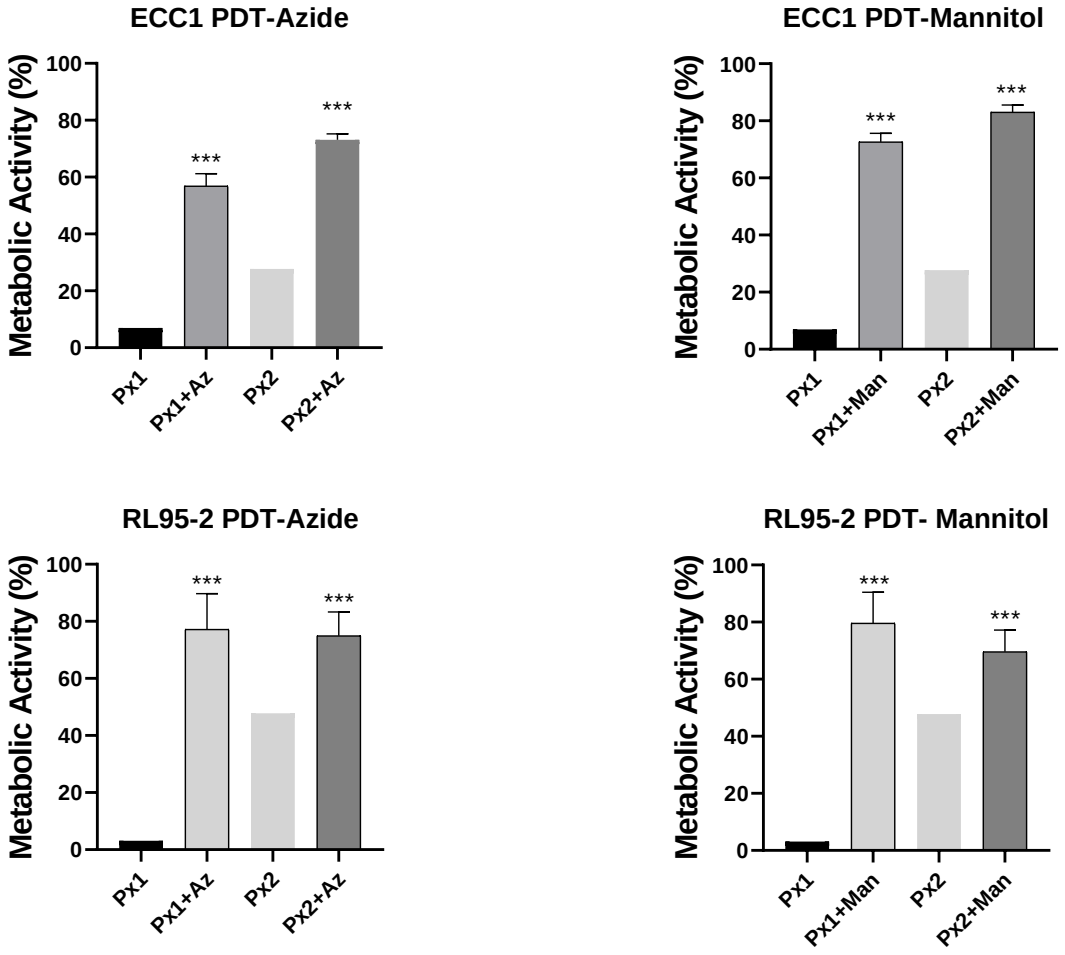

Figure 14: Photocytotoxicity of Px1 and Px2 in ECC-1 and RL95-2 endometrial cancer cells in the presence of a singlet oxygen quencher (5mM NaN_3) and a hydroxyl radical scavenger (40 mM D-mannitol). PDT was performed using the photosensitizer in a concentration of 100nM, a drug-light interval of 24 hours and irradiation with 10J. The results represent the mean and SEM of at least three independent assays. Statistically significant differences relative to cell cultures treated in the absence of the inhibitors are represented with * for $p<0.05$, ** for $p<0.001$ and *** for $p<0.0001$.

Section 2

1. PS localization in endometrial CSC

Through a confocal microscopy experiment, it was possible to observe that the photosensitizer Px1 was internalized by ECC-1 spheres, as illustrated in the following Z-Stack panel of Figure 15.

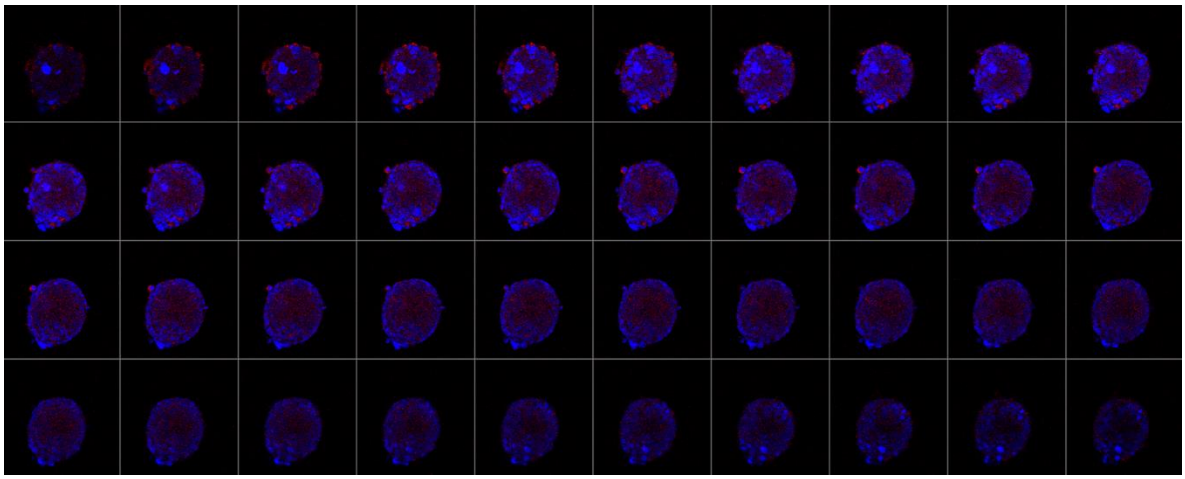

Figure 15: Confocal microscopy images of ECC-1 CSC showing the subcellular location of the photosensitizer at the periphery and the centre of the colony. Z-Stack images were taken after 24 hours of incubation with 500 nM Px1. The nuclei are stained in blue and Px1 shows its red fluorescence. Images were obtained from the bottom to the top of the ECC-1 sphere by confocal microscopy with a 400x magnification.

2. Trypan Blue assay

The viability of endometrial CSC after Px-PDT is shown in Figure 16. Regarding Px1-PDT, it was observed the significant decrease of CSC viability was in both times of incubation, 4h and 24h ($p<0.0001$) in the 500 nM and 1000 nM concentrations compared to untreated cells. Regarding Px2-PDT, it was observed a significant decrease of cell viability in both times of incubation ($p<0.0001$) in the 500nm and 1000nm concentrations compared to untreated cells.

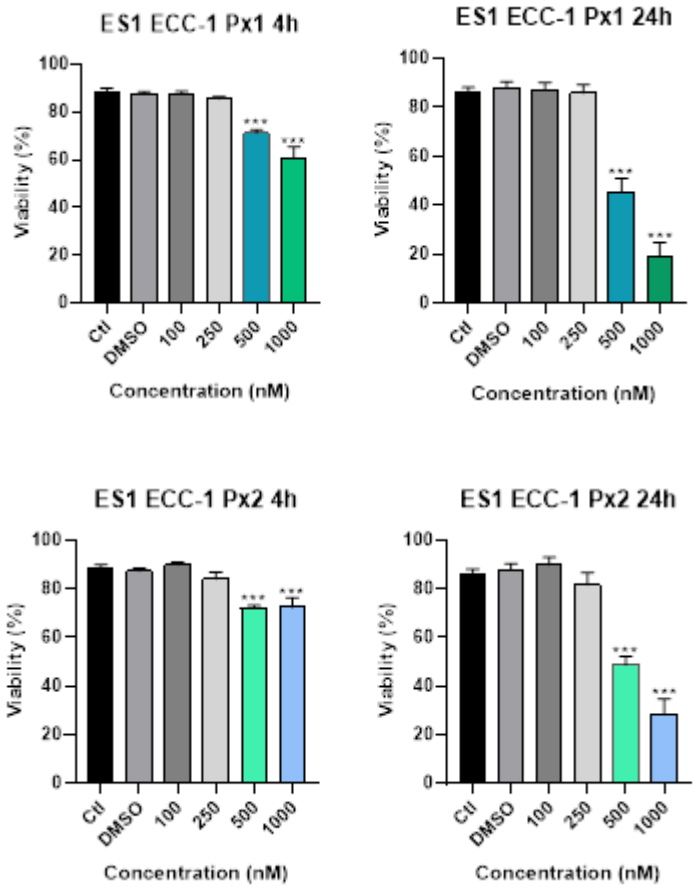

Figure 16: ECC-1 CSC cell viability evaluated using Trypan Blue exclusion method. For this study PDT, a drug-light interval of 4 or 24 hours was tested and irradiated with 10J. The results represent the mean and SEM of at least three independent assays. Statistically significant differences are represented with * for $p<0.05$, ** for $p<0.001$ and *** for $p<0.0001$

3. Metabolic activity

The metabolic activity of ECC-1 CSC was also analyzed as represented in Figure 17. Regarding Px1-PDT, the cell viability decreased from 250nM for a mean of 78,76±6.12% ($p<0.05$), For the concentrations of 500nM and 1000nM a metabolic activity of 67.80±7.41% ($p<0.01$) and 46.44±3.99% ($p<0.001$) was obtained, respectively. Regarding Px2-PDT, the cell viability decreased from concentrations of 500nM and 1000nM to metabolic activity values of 55.28±7.79% ($p<0.01$) and 29.38±6.74% ($p<0.01$), respectively.

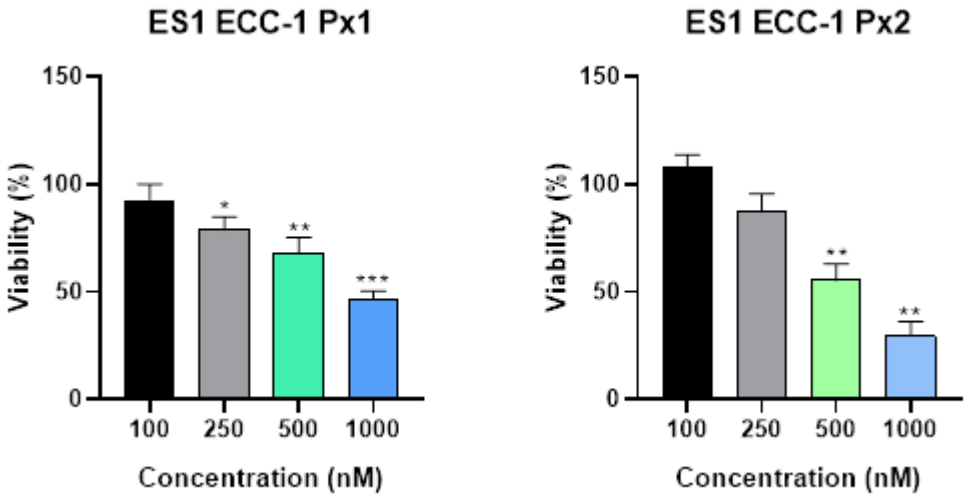

Figure 17 - ECC-1 CSC metabolic activity evaluated using Alamar Blue® assay. For this study PDT, a drug-light interval of 24 hours was tested and irradiated with 10J. The results represent the mean and SEM of at least three independent assays. Statistically significant differences are represented with * for $p<0.05$, ** for $p<0.001$ and *** for $p<0.0001$.

4. Sphere's projection area

The representative projection area of the spheres 24h after Px1-PDT is shown in Figure 18. The graphs of Figure 19 show the average projection area in pixels of the spheres, 4 and 24 hours after being submitted to Px-PDT.

In the case of Px1-PDT, 4 hours after treatment it was still not possible to discriminate statistical differences. However, 24 hours later a significant decrease of the projections areas was observed for the concentrations of 250 nM (0,6835±0,06181 pixels; $p<0.05$), 500 nM (0.2338±0.013 pixels; $p<0.001$) and 1000 nM (0.1694±0.011 pixels; $p<0.001$), while the control CSC showed an average of 1,006±0,05370 pixels.

When PDT was based on Px2 a significant decrease of projection area was observed for the higher concentration studied, 4 hours after treatment (0.4842±0.066; $p<0.01$). Px2 caused a statistically significant decrease in the area, 24 hours after treatment, starting at 500nM with a mean of 0.2427±0.017 pixels ($p<0.001$), and 1000nM with a mean 0.1867±0.012 pixels ($p<0.001$).

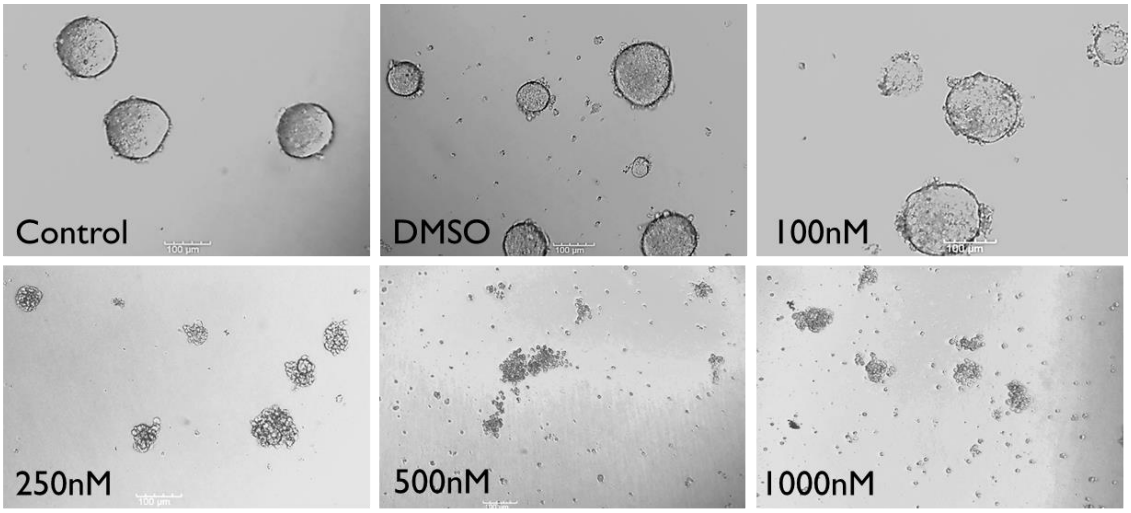

Figure 18. Representative images of the ECC1 CSC were submitted to Px-PDT. For this study, a drug-light interval of 24 hours and irradiation with 10J was performed. Images were obtained with a magnification of 100x.

.

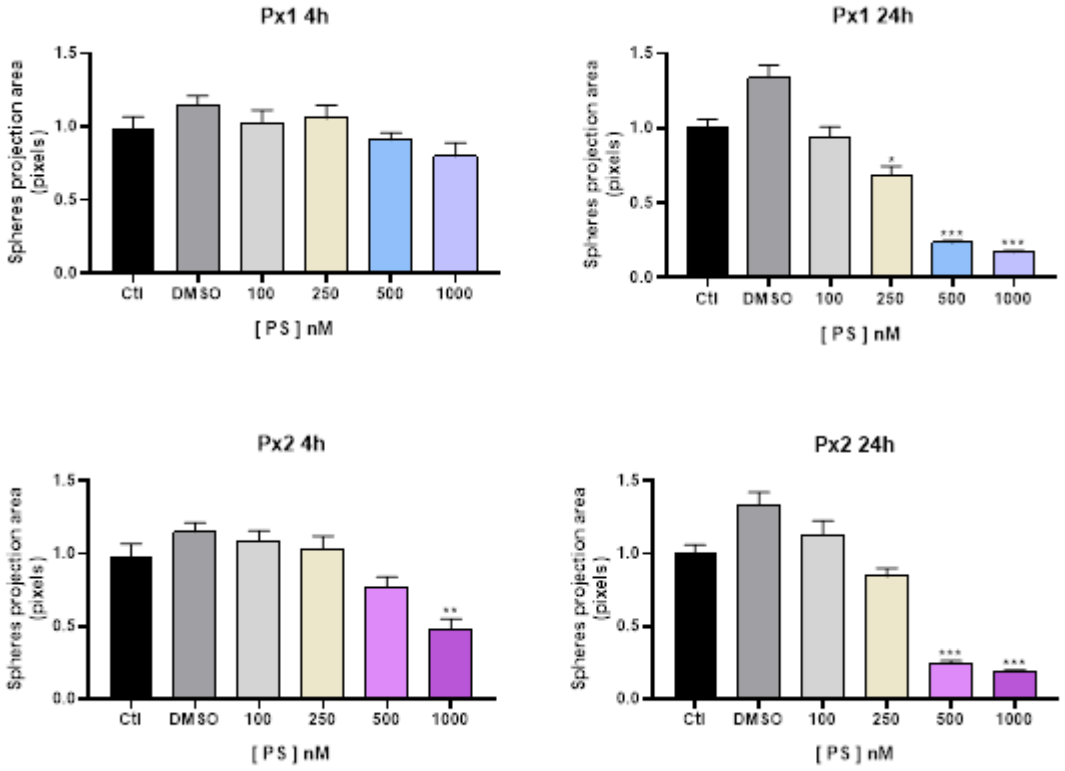

Figure 19 - Average area of ECC-1 CSC after Px-PDT. For this study PDT, a drug-light interval of 4 or 24 hours was tested and irradiated with 10J. The results represent the mean and SEM of at least 60 images for each condition obtained in at least two independent tests. Statistically significant differences are represented with * for $p<0.05$, ** for $p<0.001$ and *** for $p<0.0001$.

5 – Discussion and Conclusions

Our team has developed a group of new highly stable photosensitizers, 5-tetrahydropyrazolo[1,5-α] pyridine fused chlorins (named Px) to be used in photodynamic therapy (PDT). The photocytotoxicity of Px has been studied in a variety of cancer models, including melanoma, oesophagus and bladder cancer cells, mice, and chick chorioallantoic membrane[1–3]. The major focus of the present research was to determine if Px-PDT is effective *in vitro* as a conservative treatment for EC. For this purpose, two human endometrial cancer cell lines were used, the ECC-1 and RL95-2 cell lines.

The MTT assay consists of a yellowish solution made up of a water-soluble tetrazolium salt. This salt is absorbed by cells and reduced, mostly by mitochondrial enzymes, to generate dark blue formazan crystals. Since this molecule is impermeable to the cell membrane, it will accumulate inside living cells. Cells' capacity to reduce the MTT is a test for mitochondrial integrity and activity, which may be used to calculate metabolic activity, and, as a result, cell viability.

This assay allowed us to discover the IC_{50} values. Px1 concentrations were found to be lower in both cell lines, thus, this seems to be the most promisor PS. Nevertheless, both PS had IC_{50} values up to only 100 nM.

There is a slight but fundamental difference in the structure of Px1 versus Px2. The centre of Px2 is a Pt atom, which leads to this PS despite having a greater IC_{50} than Px1 does, to offer a multivalent component. It was previously demonstrated that it can be used in melanoma theranostics[5]. Theranostics, or the combination of imaging and therapy in a single system, allows for concurrent image-guided therapy and early follow-up of the treatment outcome, increasing treatment efficiency[2].

During high-grade glioma (HGG) surgery, for example, has been implemented fluorescence-guided surgery (FGS) employing 5-aminolevulinic acid (5-ALA) in a frequently and utilized approach for distinguishing tumour tissue from the adjacent brain intraoperatively[6]. Thus, it has been demonstrated to enhance greater increase removal rates as well as overall patient survival when used to distinguish tumour from adjacent brain tissue[6]. So, in association, there is also this hypothesis of a therapeutic potential to irradiate and apply PDT in this clinical situation.

Despite its complicated biology features, PDT has several advantages. Since the photodynamic reaction happens only when irradiation is given, photocytotoxicity effects

are local and selective. To address this, the metabolic activity of cell cultures that were not exposed to irradiation was also analyzed. Px1 and Px2 cytotoxicity in concentrations from which are up to 10x higher than the working doses of these compounds were studied, proving the safety of the sensitizers. Nevertheless, previous studies without irradiation demonstrated that the cytotoxicity is light and light dose dependent[1].

The photosensitizer uptake and its internalization evaluation are extremely important for understanding the dynamics of molecule entry and retention, which is going to impact, directly, the ideal irradiation time of PDT, after sensitizer administration. Furthermore, the subcellular location itself determines the severity of the effects and has an impact on the types of cell death7. In this work, we chose to evaluate the uptake and subcellular location of the Px1 due to its spectrophotometric characteristics[1–3]. The analysis was carried out utilizing confocal fluorescence microscopy and fluorimetry; however, some limitations in the cell study were observed in the latter.

The uptake peak in ECC-1 was 24 hours, but in RL95-2, the process is quicker, with the maximum at 8 hours, according to the periods investigated. However, as explained previously, these data must be carefully examined since just one experiment was conducted due to practical restrictions. Given that just one experiment could be conducted, such results may be attributed to a lack of confidence. However, regarding confocal microscopy studies, it was possible to observe the internalization of the compound in both lines, 24h after incubation. Confocal laser scanning fluorescence microscopy has made determining the intracellular location of PS significantly easier, and it has higher sensitivity and resolution than non-confocal methods.

Px1 shows a significant absorption by EC tumour cells, accumulating in the cytoplasm, but it does not permeate the nucleus, indicating that it cannot probably pass through the nuclear membrane. The PS's interaction with cells in the target tissue or tumour is the most essential element determining the result of PDT, and the PS's subcellular localization is a crucial piece of this interaction. PS is found in mitochondria, lysosomes, the endoplasmic reticulum, the Golgi apparatus, and plasma membranes, among other places8. Thus, it is of paramount importance in the future to understand the distribution of the photosensitizer in the cell. In the same way that DAPI is used to locate the nucleus, it would be interesting to use markers from other organelles.

Teiten *et al*. used confocal microscopy and microspectrofluorometry to investigate Foscan subcellular distribution in the MCF-7 human breast cancer cell line. Foscan has

modest distribution in lysosomes and a weak concentration in mitochondria, according to fluorescence topographic profiles obtained after cells were co-stained with Foscan and organelle-specific fluorescent probes. The Foscan fluorescence topographic profile, on the other hand, is fully co-localized with that of the endoplasmic reticulum (ER) and the Golgi apparatus. The fluorescence patterns obtained from confocal microscopy experiments were consistent with Foscan's predominant localization in these organelles[7,8].

Moreover, it would be interesting to evaluate the uptake and intracellular distributions of Px1 in endometrial non/malignant cells. According to previous *in vitro* and *in vivo* experiments[9], the endometrial and myometrial protoporphyrin IX was preferentially taken up by the cancer cells[9,]

Flow cytometry was used to examine cell viability and distinct forms of induced cell death, as well as mitochondrial membrane potential (ΔΨm), 24 hours after PDT treatment, by doubly labelling the cells with annexin V (AV) stained with the fluorescein isothiocyanate fluorochrome (FITC) and PI. In terms of apoptosis, ΔΨm is a significant event. The fluorescent dye JC-1 (5,5′,6,6′-tetrachloro-1,1′,3,3′-tetraethyl-imidacarbocyanine iodide) can be used to test it [36].

In the present study, in both ECC-1 and RL95-2 cell lines incubated with Px1-PDT at 24 hours, was induced cell death. In ECC-1 was observed late apoptosis and necrosis, and in RL95-2 mostly apoptosis. Regarding Px2-PDT, in RL95-2 cells, cell death was not so prominent, being significant by necrosis. In parallel, there was a disruption of the mitochondrial membrane potential with Px1-PDT. In this work, was observed a disturbance after PDT treatment with Px1-PDT, which led to a significant loss of mitochondrial membrane potential in ECC1 and RL95-5 cells. However, no significant changes were observed when cells were submitted to PDT based on Px2.

The collapse of mitochondrial membrane potential (ΔΨ) is one of the early stages, if not the cause, of apoptosis[36]. The electron transport chain activity and mitochondrial function are determined by the mitochondrial membrane potential. Furthermore, when the mitochondrial membrane potential is disrupted, pro-apoptotic elements such as cytochrome C are released into the cytoplasm [36]. The results obtained confirm that Px2 is less active than Px1. Regarding Px1, we verified that the type of cell death depends on the cell line studied.

Additionally, in HEC1-B human endometrial carcinoma cells, apoptosis occurred mainly at doses between 2 and 5 J/cm^2, whereas necrosis prevailed above 6 J/cm^2 in Hypericin-PDT treatment11. As observed in other studies, with all examined chlorins, a

perturbation was found following PDT treatment, and the disturbance (membrane mitochondrial potential ΔΨm) becomes more significant, with a more prominent impact reported for specific chlorins developed3. Previous work shows the type of cell death can be dependent on the concentration of the photosensitizer particularly on chlorin type.

The cell cycle analysis revealed significant retention in the G0/G1 phase in ECC-1 and RL95-2 treated with PDT- Px1 and PDT-Px2, respectively, which is consistent with the previously observed reduction in cell viability. There is a cytotoxic effect due to the increase in the G0/G1 apoptotic peak, however, there is no cytostatic effect induced by the PS, as there is a decrease in the S phase.

Oxidative stress is fundamental in PDT treatment. Therefore, the implication of several ROS in the PDT, based on the photosensitizers Px1 and Px2, was also studied.

In PDT, singlet oxygen is frequently considered the most important ROS. Considering it was unable to determine its intracellular levels directly following PDT using Px1 and Px2 photosensitizers, studies were performed in the presence of a specific inhibitor. The quencher of this oxygen reactive species, sodium azide, was utilized. Similarly, experiments were carried out in the presence of D-mannitol, a hydroxyl radical scavenger. Nevertheless, the evaluation of superoxide radical and hydroxyl production was performed using the DHE and DCF probes, respectively.

The singlet oxygen and hydroxyl radical production analysis showed the important correlation with PDT treatment. In ECC-1 and RL95-2 cells, both sodium azide and D-mannitol significantly reduced PDT's photocytotoxicity with both PS. Thus, was demonstrated that singlet oxygen production is crucial for photodynamic activity with these photosensitizers, especially regarding its role in type I reaction on PDT. Nevertheless, type II reaction is also relevant as the importance of hydroxyl species was demonstrated. Moreover, in RL95-2 cells, was observed an increased ratio of anion superoxide compared with control, and ECC-1 cells. Previous studies in our group demonstrated similar results in melanoma cells[5,13].

CSCs are part of a tumour that can self-renew, are tumorigenic, and also have the potential to resist treatments[14–16]. The multicellular tumour spheroid model was first reported in the 1970s, based on the suspension of cells cultured in a medium supplemented with fetal bovine serum but without growth hormones and cultured under non-adherent culture conditions. Several versions of this approach have been implemented over the years[17] to isolate CSC.

In this work, and following the previous research from the group18 endometrial spheres were obtained through a sphere formation protocol under non-adherent conditions. In a culture medium with methylcellulose and without bovine serum, which also helps to preserve the conditions in suspension, and supplemented with growth factors, namely EGF and bFGF[18].

CSC have particular characteristics, crucial in tumour biology, their proliferative potential, self-renewal, differentiation, and tumour migration, invasion, and metastatic capacity, tumorigenesis, and maintenance[19]. So, if therapies are targeted to these cells, the cancer niche would be destroyed, since the occurrence of a subpopulation of CSC that is innately more resistant to diverse therapy is a plausible reason for tumour resistance. The second goal of this work was to evaluate the novel photosensitizer-based PDT specifically in endometrial CSC. In this work, therefore, for the first time, these chlorine-based compounds were evaluated in 3D cell models, such as spheres.

It is already shown that endometrial cancer cell lines uptake Px1; that was demonstrated using monolayer cell cultures. While conducting the experiments leading to this dissertation, a question arises: would the PS be able to localize in whole cells that constitute a 3D sphere. Using the same methodology, confocal microscopy, in this case using a Z-Stack tool, it was possible to observe the 3D localization of Px1. Similar to what happened in the cell lines, the Px1 does not seem to enter the nucleus. Moreover, it was confirmed the subcellular location of the photosensitizer at the periphery and the centre of the sphere.

These ECC-1 spheres were submitted to Px1-and Px2-PDT to evaluate the metabolic activity of endometrial CSC to PS. The Alamar blue technique was used because it proved to be a more suitable methodology for cells in suspension. In addition, in fact, in this work, both MTT and XTT techniques were tested for this purpose, however, these techniques were not able to discriminate the differences between the conditions.

It was found that the metabolic activity decreased with increasing concentration, with a significant decrease from 250 nM for Px1 and 500 nM for Px2. In a first analysis, also in CSC, there is a greater effect of Px1 concerning Px2.

We found that the concentrations of PS necessary to decrease the metabolic activity of the spheres were higher than in the previously presented studies. To confirm these results, two studies were carried out: Trypan Blue and Spheres projection area. Both these studies were carried out with 4 and 24 hours of incubation of the PS. CSC

viability was decreased in both times of incubation, 4h and 24h, with 500 nM and 1000 nM, compared with untreated CSC, using trypan blue.

As for Trypan Blue single cells had to be obtained, we also wanted to confirm the effect on the viability of the entire spheres, taking into account the maintenance of the 3D model. Thus, in order to investigate the direct influences of PDT on CSC, the average projection area occupied by the spheres in Px1 and Px2 was evaluated. These data revealed that the projection area was mainly reduced in 24h of incubation. Px1 caused a statistically significant decrease in the area of the spheres with 250 nM, 500nM and 1000nM. For Px2, statistically significant results were seen for 500 nM and 1000 nM. In fact, the representative images in Figure 18 clearly show the alteration of the morphology and projection area of the spheres compatible with the loss of viability.

These findings suggest that Px-PDT in CSC has a potential feature similar to EC therapy, but with greater PS concentrations, since CSC appear to be less sensitive than EC cells.

Anticancer drug activity has typically been assessed in two-dimensionally (2D) grown cancer cell lines. However, it is now understood that two-dimensionally cultivated cells are unable to replicate the microenvironment of the original tumours, which develop in three dimensions (3D) [20,21.] Certain breast cancer cell lines established dense 3D-MCSs, and the generation of MCSs was linked to lower chemotherapeutic drug sensitivity[21], according to Imamura *et al*. Furthermore, findings demonstrated that drug resistance in MCSs may be produced by hypoxia, which was linked to an increase in cell population in the G0 phase and/or downregulation of pro-apoptotic molecules such caspase-3. In this approach, 3D-culture systems are more effective than 2D-culture systems in simulating the *in vivo* tumour microenvironment. Furthermore, Sullivan *et al.* found that hypoxia caused an increase in the G0 non-cycling population in breast cancer cell lines, which was linked to etoposide resistance[20,21.]

The possibility to use PDT effectively in cancer cells including CSC can be a solution to resistant cancer cells since these cells are mainly responsible for the maintenance of cancer disease[22].

Considering the significant side effects and limited efficacy of standard oncology treatments, new options are continually being presented and searched. Among these, PDT stands out, and its potential in EC treatment.

PDT is an approach that is ambulatory and may be used in conjunction with other therapeutic options. Moreover, can have a role as minimally invasive treatment in

superficial lesions or at accessible cavities, as endometrium, particularly attractive for PDT, since it is a high turnover tissue and has cyclic cell modifications50 The use of PDT to treat endometrial cells responsible for tumour initiation has the potential to be both safe and selective. Prior research has shown preferential accumulation of photosensitizers in endometrial lesions, which has been systematized in various studies[24–27].

Conclusions

The *in vitro* photodynamic impact of Px1 and Px2 photosensitizers was shown to be promising for therapeutic use, with IC50 values in the nanomolar range in EC. Despite the need of higher concentration CSC are also susceptible. Both studied chlorins are active against endometrial cancer cell lines ECC-1 and RL95-2, but Px1 has shown greater activity. Moreover, very low cytotoxicity against these cells in the absence of light activation, was observed. PX1 show a significant absorption by EC tumour cells and the 3D model of CSC, accumulating in the cytoplasm, but it does not permeate the nucleus, indicating that it cannot probably pass through the nuclear membrane. It was found that the lesion following photosensitizer-based PDT Px1 is caused not only by singlet oxygen produced by type II photodynamic reactions but also by ROS produced by type I reactions.

The results obtained in this work encourage further studies of Px based PDT in endometrial cancer.

6 - References

1. Fortner, R. T. *et al.* Theoretical potential for endometrial cancer prevention through primary risk factor modification: Estimates from the EPIC cohort. *International Journal of Cancer* **147**, 1325–1333 (2020).
2. Garzon, S. *et al.* Fertility-sparing management for endometrial cancer: review of the literature. *Minerva medica* **112**, 55–69 (2021).
3. Colombo, N. *et al.* ESMO-ESGO-ESTRO Consensus Conference on Endometrial Cancer: Diagnosis, Treatment and Follow-up. *International Journal of Gynecologic Cancer* **26**, 2–30 (2016).
4. Laranjo, M. *et al.* Platinum(II) ring-fused chlorins as efficient theranostic agents: Dyes for tumor-imaging and photodynamic therapy of cancer. *European Journal of Medicinal Chemistry* **200**, (2020).
5. Marquardt, R. M., Kim, T. H., Shin, J. H. & Jeong, J. W. Progesterone and estrogen signaling in the endometrium: What goes wrong in endometriosis? *International Journal of Molecular Sciences* vol. 20 (2019).
6. Lee, N. K. *et al.* Prognostic factors for uterine cancer in reproductive-aged women. *Obstetrics and Gynecology* **109**, 655–662 (2007).
7. Colombo, N. *et al.* ESMO-ESGO-ESTRO consensus conference on endometrial cancer: Diagnosis, treatment and follow-up. *Annals of Oncology* **27**, 16–41 (2016).
8. Brooks, R. A. *et al.* Current recommendations and recent progress in endometrial cancer. *CA: A Cancer Journal for Clinicians* 258–279 (2019) doi:10.3322/caac.21561.
9. Kanapathipillai, M. cancers Treating p53 Mutant Aggregation-Associated Cancer. (2018) doi:10.3390/cancers10060154.
10. Giannone, G. *et al.* Endometrial cancer stem cells: Role, characterization and therapeutic implications. *Cancers* **11**, 1–18 (2019).
11. Allegra, A. *et al.* The Cancer Stem Cell Hypothesis : A Guide to Potential Molecular Targets. 1–26 (2014) doi:10.3109/07357907.2014.958231.
12. Murayama, T. & Gotoh, N. Drug resistance mechanisms of cancer stem-like cells and their therapeutic potential as drug targets. *Cancer Drug Resistance* (2019) doi:10.20517/cdr.2019.36.
13. Nassar, D. & Blanpain, C. Cancer Stem Cells: Basic Concepts and Therapeutic Implications. *Annual Review of Pathology: Mechanisms of Disease* **11**, 47–76 (2016).
14. Hubbard, S. A. *et al.* Evidence for cancer stem cells in human endometrial carcinoma. *Cancer Research* **69**, 8241–8248 (2009).
15. Nascimento, B. F. O. *et al.* Ring-Fused Diphenylchlorins as Potent Photosensitizers for Photodynamic Therapy Applications : In Vitro Tumor Cell Biology and in Vivo Chick Embryo Chorioallantoic Membrane Studies. (2019) doi:10.1021/acsomega.9b01865.
16. Lucky, S. S., Soo, K. C. & Zhang, Y. Nanoparticles in photodynamic therapy. *Chemical Reviews* **115**, 1990–2042 (2015).
17. Abrahamse, H. & Hamblin, M. R. New photosensitizers for photodynamic therapy HHS Public Access. **473**, 347–364 (2016).

18. Kessel, D. The role of low-density lipoprotein of photosensitizing agents in the biodistribution Photodynamic inactivation of Gram-negative problems and possible solutions bacteria : *Journal of Photochemistry and Photobiology B: Biology* **14**, 107–108 (1992).
19. Choi, M. C., Kim, G. & Hwang, Y. Y. Fertility-sparing management combined with photodynamic therapy for endometrial stromal sarcoma: a case report. *Photodiagnosis and photodynamic therapy* **11**, 533–536 (2014).
20. Mokwena, M. G., Kruger, C. A., Ivan, M. T. & Heidi, A. A review of nanoparticle photosensitizer drug delivery uptake systems for photodynamic treatment of lung cancer. *Photodiagnosis and Photodynamic Therapy* **22**, 147–154 (2018).
21. Grabow, W. Method for Determination of Singlet Oxygen Quantum Yield for new Fluorene-based Photosensitizers in Aqueous Media for the Advancement of Photodynamic Therapy. 1–73 (2004).
22. Mafalda Sofia Laranjo. Fotossensibilizadores para Terapia e Imagem em Oncologia. (2014).
23. Benov, L. Photodynamic therapy: Current status and future directions. *Medical Principles and Practice* **24**, 14–28 (2015).
24. Collin, F. Chemical basis of reactive oxygen species reactivity and involvement in neurodegenerative diseases. *International Journal of Molecular Sciences* **20**, (2019).
25. Garg, A. D., Nowis, D., Golab, J. & Agostinis, P. Photodynamic therapy: Illuminating the road from cell death towards anti-tumour immunity. *Apoptosis* **15**, 1050–1071 (2010).
26. Beltrán Hernández, I., Yu, Y., Ossendorp, F., Korbelik, M. & Oliveira, S. Preclinical and Clinical Evidence of Immune Responses Triggered in Oncologic Photodynamic Therapy: Clinical Recommendations. *Journal of Clinical Medicine* **9**, 333 (2020).
27. Laranjo, M. *et al.* 2-Bromo-5-hydroxyphenylporphyrins for photodynamic therapy : Photosensitization efficiency , subcellular localization and in vivo studies. (2013) doi:10.1016/j.pdpdt.2012.05.003.
28. Kim, S.-M., Rhee, Y.-H. & Kim, J.-S. The Anticancer Effects of Radachlorin-mediated Photodynamic Therapy in the Human Endometrial Adenocarcinoma Cell Line HEC-1-A. *Anticancer research* **37**, 6251–6258 (2017).
29. Qiang, Y., Zhang, X., Li, J. & Huang, Z. Photodynamic therapy for malignant and non-malignant diseases: clinical investigation and application. *Chinese medical journal* **119**, 845–57 (2006).
30. Ehrlich, C. E., Young, P. C. M., Stehman, F. B., Sutton, G. P. & Alford, W. M. Steroid receptors and clinical outcome in patients with adenocarcinoma of the endometrium. *American Journal of Obstetrics and Gynecology* **158**, 796–805 (1988).
31. Corti, L. *et al.* Gynecologic cancer recurrences and photodynamic therapy: our experience. *Journal of clinical laser medicine & surgery* **13**, 325–328 (1995).
32. Pereira, N. A. M. *et al.* Novel 4,5,6,7-tetrahydropyrazolo[1,5-a]pyridine fused chlorins as very active photodynamic agents for melanoma cells. *European Journal of Medicinal Chemistry* **103**, 374–380 (2015).
33. Pereira, N. A. M. *et al.* Platinum(II) Ring-Fused Chlorins as Near-Infrared Emitting Oxygen Sensors and Photodynamic Agents. *ACS Medicinal Chemistry Letters* **8**, 310–315 (2017).
34. Way, D. L., Grosso, D. S., Davis, J. R., Surwit, E. A. & Christian, C. D. Characterization of a new human endometrial carcinoma (RL95-2) established in tissue culture. *In Vitro* **19**, 147–158 (1983).

35. Nascimento, B. F. O. *et al.* Ring-Fused Diphenylchlorins as Potent Photosensitizers for Photodynamic Therapy Applications: In Vitro Tumor Cell Biology and in Vivo Chick Embryo Chorioallantoic Membrane Studies. *ACS Omega* **4**, 17244–17250 (2019).
36. Nascimento, B. F. O. *et al.* Ring-Fused Diphenylchlorins as Potent Photosensitizers for Photodynamic Therapy Applications: In Vitro Tumor Cell Biology and in Vivo Chick Embryo Chorioallantoic Membrane Studies. *ACS Omega* **4**, 17244–17250 (2019).
37. Maioli, E. *et al.* Critical Appraisal of the MTT Assay in the Presence of Rottlerin and Uncouplers. doi:10.1007/s12575-009-9020-1.
38. Darzynkiewicz, Z., Bedner, E., Li, X., Gorczyca, W. & Melamed, M. R. Laser-Scanning Cytometry: A New Instrumentation with Many Applications. *Experimental Cell Research* **249**, 1–12 (1999).
39. Cossarizza, A. & Salvioli, S. Flow Cytometric Analysis of Mitochondrial Membrane Potential Using JC-1. *Current Protocols in Cytometry* **13**, 1–7 (2000).
40. Obata, M. *et al.* In vitro heavy-atom effect of palladium(II) and platinum(II) complexes of pyrrolidine-fused chlorin in photodynamic therapy. *Journal of Medicinal Chemistry* **52**, 2747–2753 (2009).
41. Pereira, N. A. M. *et al.* Advances on photodynamic therapy of melanoma through novel ring-fused 5,15-diphenylchlorins. *European Journal of Medicinal Chemistry* **146**, 395–408 (2018).
42. Johnson, S., Chen, H. & Lo, P. HHS Public Access. **3**, 1–4 (2016).
43. Laranjo, M. *et al.* Obtaining Cancer Stem Cell Spheres from Gynecological and Breast Cancer Tumors 1 . Sphere-forming Protocol and Derived Adherent Populations from Continuous Cell. 1–12 (2020) doi:10.3791/60022.
44. Arbor, A. Stem cells in normal breast development and breast cancer. **36**, 59–72 (2003).
45. Ponti, D. *et al. Isolation and In vitro Propagation of Tumorigenic Breast Cancer Cells with Stem/Progenitor Cell Properties*. www.aacrjournals.org (2005).
46. Laranjo, M. *et al.* Obtaining Cancer Stem Cell Spheres from Gynecological and Breast Cancer Tumors 1 . Sphere-forming Protocol and Derived Adherent Populations from Continuous Cell. 1–12 (2020) doi:10.3791/60022.
47. Paiva, A., Oliveira, C., Filomena, M. & Abrantes, A. M. Mammospheres of hormonal receptor positive breast cancer diverge to triple-negative phenotype. **38**, 22–29 (2018).
48. Maragkos, G. A. *et al.* Fluorescence-Guided High-Grade Glioma Surgery More Than Four Hours After 5-Aminolevulinic Acid Administration. *Frontiers in Neurology* **12**, 258 (2021).
49. Castano, A. P., Demidova, T. N. & Hamblin Phd, M. R. Mechanisms in photodynamic therapy: part two-cellular signaling, cell metabolism and modes of cell death. *Photodiagnosis and Photodynamic Therapy* **2**, 1–23 (2005).
50. Castano, A. P., Demidova, T. N. & Hamblin, M. R. Mechanisms in photodynamic therapy: Part one - Photosensitizers, photochemistry and cellular localization. *Photodiagnosis and Photodynamic Therapy* **1**, 279–293 (2004).
51. Gannon, M. J. *et al.* Photosensitization of the endometrium with topical 5-aminolevulinic acid. *American Journal of Obstetrics and Gynecology* **173**, 1826–1828 (1995).
52. Varriale, L., Coppola, E., Quarto, M., Veneziani, B. M. & Palumbo, G. Molecular aspects of photodynamic therapy: low energy pre-sensitization of hypericin-loaded human endometrial

carcinoma cells enhances photo-tolerance, alters gene expression and affects the cell cycle. *FEBS letters* **512**, 287–290 (2002).

53. Plaks, V., Kong, N. & Werb, Z. The cancer stem cell niche: How essential is the niche in regulating stemness of tumor cells? *Cell Stem Cell* vol. 16 225–238 (2015).
54. Hardin, H. *et al.* The evolving concept of cancer stem-like cells in thyroid cancer and other solid tumors. *Laboratory Investigation* **97**, 1142–1151 (2017).
55. Economopoulou, P., Kaklamani, V. G. & Siziopikou, K. The Role of Cancer Stem Cells in Breast Cancer Initiation and Progression: Potential Cancer Stem Cell-Directed Therapies. *The Oncologist* **17**, 1394–1401 (2012).
56. Spherical Cancer Models in Tumor Biology | Elsevier Enhanced Reader. https://reader.elsevier.com/reader/sd/pii/S1476558614001948?token=D522B0F589CB187F5E1534D1E67FED1CFDD2DB705D685775FE198831BB92C3C5B217E1D97218630411E851EF0F8622F1&originRegion=eu-west-1&originCreation=20211025142249.
57. Bottaro, Larsen, B. 基因的改变NIH Public Access. *Bone* **23**, 1–7 (2008).
58. Imamura, Y. *et al.* Comparison of 2D- and 3D-culture models as drug-testing platforms in breast cancer. *Oncology Reports* **33**, 1837–1843 (2015).
59. Siegel, R. L., Miller, K. D. & Jemal, A. Cancer statistics, 2020. *CA: A Cancer Journal for Clinicians* **70**, 7–30 (2020).
60. Is, W. & Cancer, E. About Endometrial Cancer What Is Endometrial Cancer ? 1–11.
61. Wyss, P. *et al.* Photodynamic endometrial ablation: morphological study. *Lasers in surgery and medicine* **32**, 305–309 (2003).
62. van Vugt, D. A. *et al.* Photodynamic endometrial ablation in the nonhuman primate. *Journal of the Society for Gynecologic Investigation* **7**, 125–130 (2000).
63. Wyss, P., Fehr, M., van den Bergh, H. & Haller, U. Feasibility of photodynamic endometrial ablation without anesthesia. *International journal of gynaecology and obstetrics: the official organ of the International Federation of Gynaecology and Obstetrics* **60**, 287–288 (1998).

List of Figures

List of Tables

List of Abbreviations and Symbols

AnV – Annexin V

BMI – Body Mass Index

DCF - 2',7'-dichlorofluorescein

DHE - Dihydroethidium

DMEM - Dulbecco's Modified Eagle's Medium

DMSO - dimethyl sulfoxide

DNA - deoxyribonucleic acid

EC - Endometrial Cancer

EGF - epidermal growth factor

ER - endoplasmic reticulum

ES1 – Endometrial Spheres first generation

FGF - fibroblast growth factor

IC50 - concentration value for the 50% inhibition of the metabolic activity

ISC - intersystem conversion

J - coupling constant

MTT - 3-(4,5-dimethylthiazol-2-yl)-2,5-diphenyltetrazolium bromide

PBS - phosphate buffer saline

PDT - photodynamic therapy

PS - photosensitizer

ROS - reactive oxygen species

s - singlet

S0 - ground state

S1 - singlet excited state

Sn - singlet excitation states

T1 - triplet excited state

WHO - World Health Organization

ΔΨ – Mitocondrial membrane potential diference

λ - wavelength